Title: Specific targeting of pro-death NMDA receptor signals with differing reliance on the NR2B PDZ ligand.
Authors: Soriano FX, Martel MA, Papadia S, Vaslin A, Baxter P, Rickman C, Forder J, Tymianski M, Duncan R, Aarts M, Clarke P, Wyllie DJ, Hardingham GE
Journal: The Journal of neuroscience : the official journal of the Society for Neuroscience
Year: 2008 Oct 15
Volume: 28
Issue: 42
Pages: 10696-710
DOI: 10.1523/JNEUROSCI.1207-08.2008

Published in final edited form as:
J Neurosci. 2008 October 15; 28(42): 10696–10710. doi:10.1523/JNEUROSCI.1207-08.2008.

Specific targeting of pro-death NMDA receptor signals with differing reliance on the NR2B PDZ ligand

Francesc X. Soriano[1,2,#], **Marc-Andre Martel**[1,2,#], **Sofia Papadia**[1,2], **Anne Vaslin**[3], **Paul Baxter**[1,2], **Colin Rickman**[1], **Joan Forder**[4], **Michael Tymianski**[4], **Rory Duncan**[1], **Michelle Aarts**[5], **Peter Clarke**[3], **David J.A. Wyllie**[1,2], and **Giles E. Hardingham**[1,2,*]

[1]*Centre for Integrative Physiology, University of Edinburgh, Edinburgh EH8 9XD, UK.* [2]*Centre for Neuroscience Research, University of Edinburgh, Edinburgh EH8 9XD, UK.* [3]*Département de Biologie cellulaire et de Morphologie, Université de Lausanne, Lausanne, Switzerland* [4]*Department of Neurosurgery, Toronto Western Hospital, Toronto ON M5T 2S8, Canada* [5]*Centre for the Neurobiology of Stress, University of Toronto, ON M1C 1A4, Canada.*

Abstract

NMDA receptors (NMDARs) mediate ischemic brain damage, for which interactions between the C-termini of NR2 subunits and PDZ domain proteins within the NMDAR signaling complex (NSC) are emerging therapeutic targets. However, expression of NMDARs in a non-neuronal context, lacking many NSC components, can still induce cell-death. Moreover, it is unclear if targeting the NSC will impair NMDAR-dependent pro-survival and plasticity signaling. We show that the NMDAR can promote death signaling independently of the NR2 PDZ ligand, when expressed in non-neuronal cells lacking PSD-95 and nNOS, key PDZ proteins which mediate neuronal NMDAR excitotoxicity. However, in a non-neuronal context the NMDAR promotes cell death solely via JNK, while NMDAR-dependent cortical neuronal death is promoted by both JNK and p38. NMDAR-dependent pro-death signaling via p38 relies on neuronal context, although death signaling by JNK, triggered by mitochondrial ROS production, does not. NMDAR-dependent p38 activation in neurons is triggered by submembranous Ca^{2+}, and is disrupted by NOS inhibitors and also a peptide mimicking the NR2B PDZ ligand (TAT-NR2B9c). TAT-NR2B9c reduced excitotoxic neuronal death and p38-mediated ischemic damage, without impairing an NMDAR-dependent plasticity model, or pro-survival signaling to CREB or Akt. TAT-NR2B9c did not inhibit JNK activation, and synergized with JNK inhibitors to ameliorate severe excitotoxic neuronal loss in vitro and ischemic cortical damage in vivo. Thus, NMDAR-activated signals comprise pro-death pathways with differing requirements for PDZ protein interactions. These signals are amenable to selective inhibition, while sparing synaptic plasticity and pro-survival signaling.

Keywords

NMDA receptor; neuronal death; PDZ domains; Stroke; calcium; Mitochondria; neuroprotection; nitric oxide; Protein Kinase; signal transduction

[#]These authors made an equal contribution
[*]Correspondence to Giles.Hardingham@ed.ac.uk. Tel +44 131 6507961, Fax 6506527

Introduction

A high and prolonged rise in the extracellular glutamate concentration kills central neurons (Olney, 1969). During an ischemic episode, glutamate levels build up due to synaptic release and impaired and/or reversed uptake mechanisms (Camacho and Massieu, 2006), which induce Ca^{2+}-dependent cell death via excessive activation of *N*-methyl D-aspartate glutamate receptors (NMDARs) (Arundine and Tymianski, 2004). Excessive NMDAR activity can lead to cell death in other acute episodes such as mechanical trauma, and may contribute to neurodegeneration in Alzheimer's disease (Chohan and Iqbal, 2006). The destructive effects of excessive NMDAR activity are in contrast to the pro-survival effects of physiological NMDAR activity (Ikonomidou and Turski, 2002; Hardingham and Bading, 2003; Papadia and Hardingham, 2007). Elimination of NMDAR activity *in vivo* causes widespread apoptosis and enhances trauma-induced injury in developing neurons (Gould et al., 1994; Ikonomidou et al., 1999; Adams et al., 2004). In the adult CNS, NMDAR blockade exacerbates neuronal loss when applied after traumatic brain injury and during ongoing neurodegeneration (Ikonomidou et al., 2000), and prevents the survival of newborn neurons in the adult dentate gyrus (Tashiro et al., 2006). Molecular mechanisms of synaptic NMDAR-dependent neuroprotection are beginning to be elucidated (Hetman and Kharebava, 2006; Papadia and Hardingham, 2007; Zhang et al., 2007; Papadia et al., 2008). Thus, responses of neurons to NMDAR activity follow a bell-shaped curve: both too much and too little is potentially harmful. The central role of the NMDAR in CNS physiology offers an explanation as to why clinical treatment of stroke with NMDAR antagonists has failed due to poor tolerance and efficacy (Ikonomidou and Turski, 2002; Muir, 2006). It would be desirable to block pro-death NMDAR signaling in stroke, without affecting pro-survival signaling or indeed synaptic plasticity, many forms of which are mediated by NMDAR activation.

In neurons, Ca^{2+} influx through NMDARs promotes cell death more efficiently than through other Ca^{2+} channels (Tymianski et al., 1993; Arundine and Tymianski, 2004), suggesting that proteins responsible for Ca^{2+}-dependent excitotoxicity reside within the NMDAR signaling complex (NSC). A role for the NSC in mediating NMDAR-dependent death was shown in the case of the PDZ proteins nNOS and PSD-95 (Aarts et al., 2002). PSD-95 is linked to the C-terminal PDZ ligand of NR2, and also binds to nNOS. When the interaction of NR2B and PSD-95 is disrupted, the NMDAR becomes uncoupled from nNOS activation, reducing (but not eliminating) NMDAR-dependent excitotoxicity (Aarts et al., 2002). The important role of nNOS and PSD-95 above any other PDZ proteins in mediating NMDAR-dependent excitotoxicity was recently demonstrated (Cui et al., 2007).

The attractiveness of the NSC as a therapeutic target is questioned by two issues. Firstly, it is not clear whether NSC components can be disrupted without affecting pro-survival or plasticity signaling. Secondly, NMDAR-dependent cell death can be reconstituted in non-neuronal cells lacking the NSC simply by expressing NMDARs (Cik et al., 1993; Anegawa et al., 2000) which shows that certain NMDAR-induced death pathways do not require the NSC.

We have investigated both these issues with the aim of developing an effective anti-excitotoxic strategy that spares pro-survival and plasticity signaling, focusing on two key mediators of excitotoxicity: the stress-activated protein kinases (SAPKs) p38 MAP kinase and JNK (Kawasaki et al., 1997; Borsello et al., 2003; Rivera-Cervantes et al., 2004). We find that these death pathways have differing requirements for the NSC and can be disrupted to great effect *in vivo* and *in vitro* without impacting on pro-survival signaling or a model of NMDAR-dependent synaptic plasticity.

Materials and Methods

Neuronal cultures, stimulations and assessment of nuclear morphology

Cortical neurons from E21 Sprague Dawley rats were cultured as described (Bading and Greenberg, 1991) except that growth medium was comprised of Neurobasal A medium with B27 (Invitrogen), 1% rat serum, 1 mM glutamine. Experiments were performed after a culture period of 9-10 days during which neurons developed a rich network of processes, expressed functional NMDA-type and AMPA/kainate-type glutamate receptors, and formed synaptic contacts (Hardingham et al., 2001b; Hardingham et al., 2002). Prior to stimulations, neurons were transferred from growth medium to a medium containing 10% MEM (Invitrogen), 90% Salt-Glucose-Glycine (SGG) medium ((Bading et al., 1993), SGG: 114 mM NaCl, 0.219 % $NaHCO_3$, 5.292 mM KCl, 1 mM $MgCl_2$, 2 mM $CaCl_2$, 10 mM HEPES, 1 mM glycine, 30 mM glucose, 0.5 mM sodium pyruvate, 0.1 % Phenol Red; osmolarity 325mosm/l). Neurons were treated with NMDA in the presence or absence of tetrodotoxin (TTX, 1 μM, Calbiochem). To trigger NMDAR-dependent excitotoxic cell death, neurons were exposed to NMDA or glutamate (in the presence of nifedipine (5 μM, Tocris, Ellisville, MO)) in our standard trophically deprived medium (90% SGG, 10% MEM) for 1 h, after which neurons were washed once and returned to fresh medium. Neurons that die in response to exposure to excitotoxic levels of glutamate exhibit swollen cell bodies and pyknotic nuclei with small irregular chromatin clumps, a characteristic of necrotic cell death as opposed to apoptotic-like death ((Fujikawa et al., 2000), see (Hardingham et al., 2002) for example pictures). Cell death was determined 24 h later by counting the number of DAPI-stained pyknotic/necrotic nuclei as a percentage of the total. For each treatment, 800-1000 cells were scored across several random fields within 3-4 independent experiments. When used, FCCP (1 μM) + oligomycin (10 mM) were added 5 min before stimulation. TAT-based peptides were used at 2 mM and were added 1 hour before stimulation, as were all pharmacological inhibitors. MitoQ (10-(6′ubiquinoyl decyltriphenylphosphonium bromide) and its decyltriphenylphosphonium bromide (DTPP) targeting moiety control (gifts from Dr Mike Murphy, University of Cambridge) were used at 5 μM and added 1 h prior to stimulation.

Transfection and luciferase assays

AtT20 cells (ECACC no 87021902) were maintained in D-MEM medium (Invitrogen, Paisley, UK) supplemented with 10% Fetal Bovine Serum (Invitrogen) and antibiotics. AtT20 cells were transiently transfected in 24-well plates with pCis vectors containing full length mouse cDNAs encoding for the NR1-1a (hereafter referred to as NR1) and NR2B subunits, along with a SV40-luciferase plasmid in a 2:2:1 ratio, respectively. Transfection was done using a total of 0.5 μg cDNA/well and 2.33 μl/well of Lipofectamine reagent (2μg/ml) or Lipofectamine 2000 (1 μg/ml, both from Invitrogen). Transfection was achieved following the manufacturer's instructions and using the OptiMEM I medium (Invitrogen). Transfection efficiency was approximately 5-10%. At the end of the transfection period, the mixture was replaced with fresh OptiMEM I containing 50 μM D-APV (Tocris) to prevent spontaneous NMDAR-induced cell death. Assays were performed 16-24 h after the end of transfection. Transfected AtT20 cells were stimulated with various glutamate concentrations for 5-7 hours, with drugs being pre-applied for at least 1 hour prior to agonist application. After the incubation period, the medium was removed and 90 μl of Steady Glo luciferase assay kit (Promega, Madison, WI) mixture was added to an equal amount of fresh medium. Cells were allowed to lyse at room temperature for 10 minutes, then transferred to opaque white 96-well plates (Greiner Bio-One, Stonehouse, UK). Luciferase activity was measured by assaying the chemiluminescence using FLUOstar Optima plate reader (BMG Labtech, Offenburgh, Germany). The relative light units were converted to percentage of cell death compared to control (100%) and the minimum luminescence value was normalized to 0% to account for transfection efficiency variations.

To confirm the existence of functional NMDARs in the transfected AtT20 cells, recordings of agonist-evoked whole-cell currents in NMDAR-expressing AtT20 cells were made 18-72 h after transfection using a Mg^{2+}-free external solution. Agonists (100 μM glutamate + 100 μM glycine) were applied with an independent line positioned near the whole-cell clamped cell to achieve quick stimulation and to minimize exposure of adjacent cells to agonists. Data were filtered at 1 kHz and digitized at 5 kHz for subsequent off-line analysis.

Neurons were transfected at DIV8 using Lipofectamine 2000 as described (Mckenzie et al., 2005). Transfection efficiency was approximately 2-5 %. >99% of eGFP-expressing transfected neurons were NeuN-positive, and <1% were GFAP positive (Papadia et al., 2008) confirming their neuronal identity. For CRE-reporter assays, neurons were treated with bicuculline 24 h after transfection with 0.5 μg of CRE-Luc + 0.1 μg of pTK-renilla. Bicuculline-induced activity was terminated (by MK-801 and TTX) after 30 min or 1 hand luciferase expression analysed 6-7 h later. Luciferase assays were performed using the Dual Glo assay kit (Promega) with Firefly luciferase-based CRE-reporter gene activity normalized to the Renilla control in all cases.

^{45}Calcium assay: measurement of total, cytoplasmic and vesicular Ca^{2+} loads

5 μM nifedipine was added 1 hour prior to experiment to prevent calcium entry through voltage-gated calcium channels. Cortical neurons and NMDAR-expressing AtT20 cells were then stimulated for 10 minutes at 37°C with glutamate, using medium enriched with 30-50 MBq/L of $^{45}Ca^{2+}$. After the 10 minutes incubation, cells were washed once with fresh medium supplemented with kynurenate (10 mM) and magnesium (10 mM). For measuring total Ca^{2+} load cells were simply lysed with phosphate buffer saline (PBS) containing 1% Triton and transferred to scintillation vials. To measure cytoplasmic and vesicular Ca^{2+} load separately, we followed an established procedure (Ward et al., 2005). Briefly, cytoplasmic Ca^{2+} was released from the cells by adding 100 μl of Ca^{2+}-free medium containing 0.01% digitonin for 2 min, then collected for counting. The remaining vesicular Ca^{2+} was then measured by adding PBS/Triton as before. After addition of 1 ml of scintillation liquid (VWR), Ca^{2+}entry in counts per minute (CPM) was quantified using a Beckman LS6500 scintillation counter. Data from each experiment were normalized for the amount of $^{45}Ca^{2+}$ activity used and the basal radioactivity count from the non-stimulated cells was subtracted from each subsequent condition.

Recordings and analysis of mEPSC and sEPSC frequency

For miniature excitatory postsynaptic currents (mEPSCs) recordings, neurons were placed in medium containing control solution ± 50 μM bicuculline (Tocris) for 15 min, then returned to control medium for 30 min. Coverslips were then transferred into a recording chamber containing artificial cerebrospinal fluid (aCSF) made of (in mM): 150 NaCl, 2.8 KCl, 10 HEPES, 2 $CaCl_2$, 1 $MgCl_2$ and 10 glucose, pH 7.3 (320-330 mOsm). Patch pipettes were made from thick-walled borosilicate glass (Harvard Apparatus, Kent, UK) and filled with a K-gluconate-based internal solution containing (in mM): 155 K-gluconate, 2 $MgCl_2$, 10 Na-HEPES, 10 Na-PiCreatine, 2 Mg_2-ATP and 0.3 Na_3-GTP, pH 7.3 (300 mOsm). These electrodes were coated with Sylgard 184 resin (Dow Corning, Midland, MI) and their tips were fire-polished for a final resistance between 5-10 MΩ.

MEPSCs were recorded (Baxter and Wyllie, 2006) using an Axopatch-1C amplifier (Molecular Devices, Union City, CA) at room temperature (21 ± 2°C) with the aCSF supplemented with 300 nM tetrodotoxin (TTX) and 50 μM picrotoxin (PTX, both from Tocris). Events were recorded for 5-10 minutes (minimum of 300 events) from neurons clamped at −70 mV. Recordings were rejected if the cell holding current was higher than −100 pA or if series resistances drifted by more than 20% of their initial value and were less than 35 MΩ. For data

analysis, the tape-recorded mEPSCs were filtered at 2 kHz and digitized at 10 kHz using WinEDR v6.1 software (John Dempster, University of Strathclyde, UK). Files were then analyzed as described previously (Baxter and Wyllie, 2006) with MiniAnalysis software (Synaptosoft, Fort Lee, NJ). mEPSCs were manually selected with a minimum amplitude threshold of 6 pA (approximately 2 times the baseline noise level) and a maximum peak rising-time threshold of 5 ms.

Recordings of spontaneous EPSCs (sEPSCs) were obtained using an aCSF with 3 mM of $CaCl_2$ in order to obtain a reliably high level of spontaneous events in the cultures. Activity was recorded for 3 min whilst holding the neuron at −70 mV. Only sEPSCs greater than 200 pA and spaced by more than 1 sec were selected for frequency analysis.

Western blotting and antibodies

Total cell lysates were boiled at 100°C for 5 min in 1.5x sample buffer (1.5M Tris pH 6.8; Glycerol 15%; SDS 3%; β-mercaptoethanol 7.5%; bromophenol blue 0.0375%). Gel electrophoresis and western blotting were performed using the Xcell Surelock system (Invitrogen) with precast gradient gels (4-20%) according to the manufacturer's instructions. The gels were blotted onto PVDF membranes, which were blocked for 1 hour at room temperature with 5% (w/v) non-fat dried milk in TBS with 0.1% Tween 20. The membranes were incubated at 4°C overnight with the primary antibodies diluted in blocking solution: Anti-phospho-Jun Ser73 (1:500, Cell Signaling), phospho-Jun Ser63 (1:500, Cell Signaling), Jun (1:1000; BD Transduction Laboratories), phospho-p38 Thr180/Tyr182 (1:400, Cell Signaling}, p38 (1:1000, Santa Cruz) b-tubulin isotype III (1: 125000, Sigma), Phospho-Akt Ser473 (1:500, Cell Signaling), Akt (1:500, Cell Signaling), p-ASK1 Thr845 (1:1000, Cell Signaling), p-MKK4 Thr261 (1:1000, Cell Signaling), HA (1:1000, Cell Signaling), p-p44/42 MAPK Thr2002/Tyr204 (p-ERK1/2; 1:2000, Cell Signaling), PSD-95 (1:1000, Abcam (goat)), nNOS (1:500, AbCam (goat)). For visualisation of Western blots, HRP-based secondary antibodies were used followed by chemiluminescent detection on Kodak X-Omat film. Western blots were analyzed by digitally scanning the blots, followed by densitometric analysis (ImageJ). All analysis involved normalizing to a loading control, either to the unmodified version of the modification under study (e.g. phospho-p38 normalized to p38) or to b-tubulin isotype III.

RNA isolation, RT-PCR and qPCR

RNA was isolated using the Qiagen RNeasy isolation reagents (including the optional Dnase treatment) following passage of the cells through a QiaShredder column. For qPCR, cDNA was synthesized from 1-3 μg RNA using the Stratascript QPCR cDNA Synthesis kit (Stratagene, Amsterdam, Netherlands) according to the manufacturer's instructions. Briefly, the required amount of RNA (up to 3 μg) was diluted in RNase-free water (up to 7 μl final volume) and mixed on ice with 1x cDNA Synthesis master mix (10 μl), random primers: oligo-dT primers 3:1 (total 2 μl- 200 ng) and either 1 μl RT/RNase block enzyme mixture (for RT reactions) or 1 μl water (for No RT control reactions). Reaction mixtures were mixed and span down and incubated for 2 min. at 25°C, 40 min. at 42 °C and 5 min. at 95°C. cDNA was stored at −20°C. Dilutions of this cDNA were used subsequently for real-time PCR (cDNA equivalent to 6 ng of initial RNA per 15 μl qPCR reaction for all genes except GAPDH; cDNA equivalent to 2 ng initial RNA per 15 μl reaction for GAPDH). qPCR was performed in an Mx3000P QPCR System (Stratagene) using Brilliant SYBR Green QPCR Master Mix (Stratagene) according to the manufacturer's instructions. Briefly, the required amount of template was mixed on ice with 1x Brilliant SYBR Green Master Mix, the required concentration of forward and reverse primers, 30 nM ROX passive reference dye and water to the required reaction volume. Technical replicates as well as no template and no RT negative controls were included and at least 3 biological replicates were studied in each case. The sequence and concentration

of the primers used are as follows: Rat Adcyap1 –F: 5′- ATGTGTAGCGGAGCAAGG-3′ 200 nM, -R: 5′- GAGTGGCGTTTGGTAAGG-3′ 200nM; rat GAPDH –F: 5′- AGAAGGCTGGGGCTCACC-3′ 200 nM, -R: 5′- AGTTGGTGGTGCAGGATGC-3′ 100 nM. The cycling program was 10 min at 95 °C; 40 cycles of 30 sec. at 95 °C, 40 sec. at 60°C with detection of fluorescence and 30 sec. at 72 °C; 1 cycle (for dissociation curve) of 1 min at 95 °C and 30 sec. at 55 °C with a ramp up to 30 sec. at 95 °C (ramp rate: 0.2 °C/sec) with continuous detection of fluorescence on the 55-95 °C ramp. The data were analyzed using the MxPro QPCR analysis software (Stratagene). Expression of the gene of interest was normalized to GAPDH, a commonly used control.

Immunoprecipitation

For each treatment, 3x35 mm dishes (approx 1.5×10^6 neurons) transfected with pHA-ASK1 or control (globin) expression vector were lysed in 400 ml of Lysis buffer (0.05M Tris Base, 0.9% NaCl, pH 7.6, 0.5% Triton X-100 plus Protease Inhibitors Cocktail Set III (1:100; Calbiochem) and phosphatase inhibitor cocktails 1 and 2 (1:500, Sigma)). Lysate was clarified at 16000g for 15 min at 4 °C. The supernatant was then precleared with 25 ml of 50% Protein A Sepharose (Sigma) for 1 hour at 4 °C and, after a brief spin, the pellet was discarded. 10% of the supernatant was retained as input for normalization purposes. The remainder was incubated over night with 1:100 dilution of anti-HA antibody (Cell Signaling) at 4°C. The immuno-complex was precipitated with 25 ml of 50% Protein A Sepharose for 1 h at 4°C. The pellet was washed 3 times in lysis buffer, then boiled for 10 min in 25 ml 1.5x sample loading buffer (1.5 M Tris, pH 6.8, 15% glycerol, 3% SDS, 7.5% b-mercaptoethanol, 0.0375% bromophenol blue) prior to gel electrophoresis and Western blotting.

Neonatal Focal ischemia models

All animal procedures were in compliance with the directives of the Swiss Academy of Medical Science and were authorized by the veterinary office of the Canton of Vaud. D-JNKI1 and Tat-NR2B9c peptides were dissolved in saline and administered intraperitoneally. Since the therapeutic time window with D-JNKI1 has been shown to be 12 h, with maximal protection at 6 h for MCAO in P14 rats, we administered D-JNKI1 at 6 h after the onset of ischemia; the chosen dose was 0.3 mg/kg i.p. since pilot experiments showed this to be optimal (A. Vaslin, unpublished). In contrast, Tat-NR2B9c (7.5 mg/kg) was given 30 min. before cerebral ischemia since the therapeutic window was unknown. Control animals received saline. Focal ischemiawas induced in 12 day old male Sprague-Dawley rats. Anesthesia was induced with 2.5% isoflurane in a chamber and maintained during the operation with a mask using 2.5% isoflurane. MCAO was performed as described (Borsello et al., 2003). A more severe model (MCAO+) was performed (Renolleau et al., 1998). Briefly, the main (cortical) branch of the left middle cerebral artery was electrocoagulatedjust below the bifurcation of the MCA into frontal and parietal branches (as per the MCAO model). The left common carotid artery was then occluded by means of a clip for 90 min., during which time the rat pups were maintained at 37°C in the induction chamber (2.5% isoflurane). The arterial clip was then removed and the restoration of carotid blood flow was verified under a dissecting microscope before the skin incision was closed. Rat pups were transferred back to their mothers for a 24 h survival period. This severe model was compared with a milder model of permanent MCAO alone. With both models, the survival rate until sacrifice was 100%.

The volume of the infarct was measured after 24 h of recirculation. Pups were heavily anesthetized with sodium pentobarbital and perfused through the ascending aorta with 4% paraformaldehyde in PBS (pH 7.4). Brains were removed, placed in PBS with 30% sucrose for about 15 h at 4°C and then frozen in isopentane(−40°C). Cryostat coronal sections of 50 μm were stained with cresylviolet. The outline of the infarct was traced in each tenth slice using a computer-microscope system equipped with the Neurolucida program (MicroBrightField)

and the infarct volume calculated with Neuroexplorer (MicroBrightField). Lesions of less than 5 mm^3 (i.e. <10% of the mean lesion volume in saline controls) were considered artifactual (due to technical error or vascular abnormality), and were eliminated from the main analysis. Three saline control rats were eliminated; however, reanalysis of the data confirmed that their inclusion would have changed none of the conclusions.

3 Pial Vessel Occlusion Model (3PVO) of Ischemia

Male Sprague Dawley rats (n = 8 in each group) weighing between 280-320 g were used for this study. Except for 12 hours immediately preceding surgery, all animals had free access to standard laboratory food before and after surgery. Experimental procedures were followed using guidelines established by the Canadian Council for Animal Care and have been approved by the UHN Animal Care Committee. Rats were anesthetized with a 0.5 ml/kg intramuscular injection of ketamine (100 mg/kg), acepromazine (2 mg/kg), and xylazine (5 mg/kg), supplemented with one third of the initial dose as required. An anal temperature probe was inserted and the animal was placed on a heating pad maintained at 37°C. The right external carotid artery (ECA) was cannulated with PE 10 polyethylene tubing for dye injections. The skull was exposed via a midline incision, scraped free of tissue, and the *temporalis* muscle disconnected from the skull on the right side. Using a dissecting microscope and a pneumatic dental drill, a 6x4 mm cranial window was made over the right somatosensory cortex (2 mm caudal and 5 mm lateral to bregma) by drilling a rectangle through the skull and lifting off the piece of skull while keeping the dura intact. The tail vein was cannulated and drugs injected in the following order: Tat-NR2B9c peptide (7.5mg/kg) or saline, 15 min prior to ischemia; p38 inhibitor SB202190 (30 mg/kg) or saline 10 min prior to ischemia. After being bathed with aCSF (maintained at 37°C), small boluses (10 to 20 μl) of the vital dye patent blue violet (10 mmol/l; Sigma) in normal saline, were injected into the right external carotid artery to demonstrate transit through surface vessels of the cortex. Three critical arteriolar branches of the MCA around the barrel cortex were selected and electrically cauterized through the dura. After the cauterizations, the bolus injections and dye transits were repeated to ensure transits through the cauterized arterioles were blocked. The rectangle of skull was replaced over the window and the scalp was sutured. The catheter was removed from the ECA, the ECA was ligated, and the anterior neck was sutured. Each rat was returned to its individual cage under a heating lamp to maintain body temperature until the rat fully recovered. Food and water was supplied ad libitum. Twenty-four hours post-surgery, animals were re-anesthetized with 1 ml pentobarbital and the brain was quickly harvested. Coronal slices (2mm) was taken through the brain and incubated in 2% triphenyltetrazolium chloride (TTC) for 15 minutes at 37 °C. Images were scanned and brain slices were stored at −80 °C.

Results

The NR2 PDZ ligand is not needed for NMDAR-mediated death in NMDAR-expressing AtT20 cells

We investigated cell death induced by NMDARs in the absence of the neuron-specific NMDAR signaling complex by expressing NR1/NR2B NMDARs in AtT20 cells(NR-AtT20 cells). The ultimate aim of these experiments is to determine how the NMDAR can signal to cell death in the absence of the neuronal NSC. Such signals are likely to be activated in neurons, in addition to signals that do require the NSC. Knowledge of both types of death signals may help in developing an effective anti-excitotoxic strategy. NR2B-containing NMDARs were chosen because the neurons used in this study for comparison are DIV9 cortical neurons whose NMDAR currents are NR2B-dominated: whole-cell NMDAR currents are inhibited by 68 ± 6% by the NR2B-specific antagonist ifenprodil (n = 6, data not shown). Pure NR1/NR2B NMDARs are inhibited by approximately 80% by ifenprodil (Tovar and Westbrook, 1999),

indicating that the majority of NMDARs in DIV9 cortical neurons are NR2B-containing. Consistent with this, ifenprodil prevents NMDAR-dependent neuronal cell death (see below).

NR-AtT20 cells were subjected to patch-clamp analysis to confirm the formation of functional NMDARs (Fig. 1a for example). For viability studies NR-AtT20 cells were co-transfected with a constitutively active luciferase vector (pSV40-Luc) which acts as a bio-assay of NMDAR-dependent death in reconstituted systems (Boeckman and Aizenman, 1996) where transfection efficiency is low (<10% in AtT20 cells). Due to a more positive resting membrane potential than neurons, spontaneous NMDAR activity can be high in NMDAR-expressing non-neuronal cells, so AtT20 cells were cultured post-transfection in 50 μM APV. Glutamate treatment caused death of NR-AtT20 cells in a dose-dependent manner by out-competing the APV (Fig. 1b), and was associated with Ca^{2+} influx (measured using a $^{45}Ca^{2+}$ tracer, Fig. 1c). Death/loss of luciferase signal was blocked by MK-801 (Fig. 1b), and expression of NR2B alone (i.e. no NR1) failed to confer glutamate-induced death on AtT20 cells (Fig. 1b), confirming the need for functional NMDARs. To confirm that loss of luciferase signal corresponded to death, we corroborated these findings by studying the glutamate-dependent loss of eGFP-expressing NR-AtT20 cells (data not shown). To further test the validity of the technique, we first confirmed that in neurons, ifenprodil protected against glutamate-induced nuclear pyknosis (Fig. 1d) as well as preventing glutamate-induced loss of luciferase signal from neurons transfected with pSV40-Luc (Fig. 1d).

We next studied the expression of PSD-95 and nNOS in AtT20 cells, since these PDZ proteins are important in coupling the NMDAR to cell death in neurons, via the NR2 PDZ ligand (Cui et al., 2007). Western blot analysis revealed that levels of PSD-95 and nNOS were extremely low in AtT20 cells, compared to levels in equivalent amounts of neuronal protein extract (Fig. 1e). This suggests that the PDZ ligand of NR2B may not be important for NMDAR-dependent cell death in NR-AtT20 cells. To test this, AtT20 cells were transfected with vectors encoding NR1 plus a truncated form of NR2B lacking the PDZ ligand, NR2Btrunc (Rutter and Stephenson, 2000). Expression of NMDARs containing NR1 and NR2Btrunc triggered the same Ca^{2+} load (Fig. 1f) and also was equally effective at promoting cell death (Fig. 1g) as wild-type NMDARs. Thus, in the non-neuronal environment of an AtT20 cell, NMDARs can couple to cell death in the absence of PSD-95, nNOS, and the NR2B PDZ ligand, all components that contribute to NMDAR excitotoxicity in neurons (Cui et al., 2007).

Differing p38 MAPK dependency of NMDAR signaling to death in neurons vs. NR-AtT20 cells

To investigate this apparent paradox, we studied the signals responsible for mediating NMDAR-dependent cell death in neurons and NR-AtT20 cells, focusing on two key mediators of excitotoxicity, the SAPKS p38 and JNK (Kawasaki et al., 1997; Borsello et al., 2003). Under basal conditions CNS neurons contain a pool of active JNK1 which does not influence viability, but can make it difficult to detect additional elevation of stress-activated JNK signaling with phospho-JNK antibodies (Coffey et al., 2002). Since this pool of JNK1 does not influence c-Jun phosphorylation, the latter was used as a sensitive metric of NMDAR-dependent JNK signaling (Fig. 2a). NMDAR-dependent c-Jun phosphorylation was inhibited by the JNK inhibitor SP600125, as well as the peptide inhibitor of JNK, D-JNKI1 (Borsello et al., 2003) (Fig. 2a), but not the p38 inhibitor SB203580 (data not shown). SP600125 did not interfere with p38 autophosphorylation, in contrast to SB203580 (data not shown). In neurons, NMDAR activation induced both p38 and JNK signaling (Fig. 2b,c). Since we did not have access to neurons from JNK and p38 isoform-deficient mice, we tested the JNK/p38 inhibitors on NMDA-induced excitotoxicity to see whether these stress-activated protein kinases play a role in excitotoxicity in our system. Inhibitors of JNK and p38 reduced NMDAR-dependent cell death (Fig. 2d), indicating a contribution from both pathways.

In contrast to the effects of both JNK and p38 inhibitors on NMDAR-dependent neuronal death, JNK inhibition completely blocked NMDAR-dependent death of NR-AtT20 cells, while p38 inhibition had no effect (Fig. 2e). This is not due to absence of the p38 pathway in AtT20 cells: known SAPK activators, H_2O_2 and anisomycin, induced p38 activation (data not shown). The absence of a p38-dependent component of NMDAR-dependent death of NR-AtT20 cells indicated that neuron-specific signaling molecules may be required for p38 activation by NR2B-containing NMDARs.

NMDAR signaling to p38 MAPK involves NOS and requires only submembranous Ca^{2+} in neurons

In cortical neurons, p38 is an important downstream effector of NO toxicity (Ghatan et al., 2000), and in cerebellar granule cells NMDAR-dependent p38 activation is NOS-dependent (Cao et al., 2005). To determine whether NMDAR signaling to p38 is NOS-dependent in cortical neurons we treated them with the NOS inhibitors L-NAME and 7-nitroindazole (in arginine-free medium). Both inhibitors impaired p38 activation by NMDA (Fig. 3a) but not by H_2O_2 treatment (data not shown), indicating that NOS activation by NMDA is upstream of p38 in cortical neurons. To determine whether NO was sufficient to induce p38 activation in cortical neurons we exposed them to the NO donor S-Nitroso-N- acetylpenicillamine (SNAP), and found efficient p38 activation (Fig. 3b) that was transient, as is NMDAR-induced p38 activation (data not shown). The transient nature of p38 activation (phosphorylation followed by dephosphorylation, Fig. S2) has been observed previously (Waxman and Lynch, 2005). The ability of NMDARs (specifically NR2B-containing NMDARs) to trigger p38 dephosphorylation (Krapivinsky et al., 2004; Waxman and Lynch, 2005) raises the question as to whether NOS inhibitors act by blocking NMDAR-dependent p38 activation, or by slowing the p38 desphosphorylation. The former is more likely: even at 1 min stimulation, which is before full induction of p38, L-NAME inhibits NMDAR-dependent p38 activation (data not shown).

While some NMDAR-dependent events such as calcineurin-dependent NFAT translocation require bulk cytoplasmic Ca^{2+} increases, others such as the Ras-ERK1/2 pathway require only submembranous Ca^{2+} increases in the immediate vicinity of the NMDAR (Hardingham et al., 2001a). A sole requirement for submembranous Ca^{2+} would indicate receptor-proximal effectors of the NOS-p38 MAPK cascade. To determine this, we used a technique we previously established involving the cell-permeable Ca^{2+} chelator EGTA-AM and bicuculline (Hardingham et al., 2001a). Brief, easily bufferable, NMDAR-dependent Ca^{2+} transients were generated by network disinhibition using $GABA_A$ receptor blockade (bicuculline). These transients activated p38 in a MK-801-sensitive manner, just like NMDA bath application (Fig. 3c). We previously showed that preloading EGTA-AM at increasing concentrations prior to bicuculline stimulation blunts global Ca^{2+} transients at low doses of EGTA-AM, and abolishes them at 100 μM EGTA-AM (Hardingham et al., 2001a). The bicuculline stimulation is needed rather than bath-NMDA because the latter saturates the EGTA buffer. Since EGTA has a slow on-rate for Ca^{2+} binding, it allows increases in Ca^{2+} very near the site of entry, so bicuculline-induced bursting, reliant on evoked neurotransmitter release (a classical membrane-proximal Ca^{2+}-dependent process) still takes place (Hardingham et al., 2001a). Thus, EGTA-AM restricts intracellular Ca^{2+} transients to the immediate vicinity of the site of entry (the NMDAR). Strikingly, EGTA-AM loading did not compromise the activation of p38 following bicuculline treatment, even at 100 μM (Fig. 3d,e). In contrast, activation of Akt, another known NMDAR-activated signaling molecule, is abolished (Fig. 3d,f). We confirmed that p38 activation by bicuculline stimulation is NMDAR-dependent (Fig. 3c) and NMDAR-dependent activation of p38 requires Ca^{2+} influx (no activation was observed in Ca^{2+} -free medium, data not shown). We conclude from Fig. 3 that Ca^{2+} elevation in the immediate vicinity of the NMDAR is sufficient to trigger NOS-dependent p38 signaling in cortical neurons.

NMDAR signaling to p38 MAPK in neurons is disrupted by a peptide mimetic of the NR2B PDZ ligand

A recent study in cerebellar granule neurons showed that uncoupling of the NMDAR-associated scaffold protein PSD-95 from associated proteins, including nNOS (by overexpressing their interaction domains) impaired signaling to p38 (Cao et al., 2005). PSD-95 associates with the NMDAR via the C-terminal PDZ ligand of NR2. To determine whether the NR2 PDZ ligand plays a role in the NOS-dependent activation of p38 signaling in cortical neurons, we treated neurons with TAT-NR2B9c, a cell permeable (TAT-fused) peptide mimetic of the 9 C-terminal amino acids of NR2B, containing the PDZ ligand. TAT-NR2B9c disrupts NR2B/PSD-95 interactions, and uncouples the NMDAR from NO production (Aarts et al., 2002). TAT-NR2B9c strongly impaired NMDAR-dependent p38 activation (Fig. 4a), without impairing NMDAR-dependent Ca^{2+} influx as assayed by $^{45}Ca^{2+}$ accumulation (Fig. S1). TAT-NR2B9c did not effect basal levels of p38 activity, nor did it effect p38 activation by a different stimulus (H_2O_2 treatment, data not shown). Thus, the effect of TAT-NR2B9c on p38 signaling appears to be specific to NMDAR-dependent p38 activation.

TAT-NR2B9c did not inhibit NMDAR-dependent activation of JNK signaling (Fig. 4b). Note that the effect of TAT-NR2B9c on p38 activation was observed at both the point of peak p38 activity (5 min, Fig. 4a) and also at 30 min (data not shown), the timepoint at which the lack of JNK inhibition was observed.

Given that NMDAR-dependent death of NR-AtT20 cells is JNK-dependent (Fig. 2e) and does not rely on the NR2 PDZ ligand (Fig. 1g), we would expect that TAT-NR2B9c would not impair NMDAR-dependent cell death of NR-AtT20 cells. This is indeed the case: TAT-NR2B9c had no effect on NMDAR-dependent death of NR-AtT20 cells (data not shown). Thus, the effect of TAT-NR2B9c on NMDAR signaling to cell death is specific to the p38 pathway, and further supports the idea that JNK signaling is independent of the NR2 PDZ ligand. Moreover, TAT-NR2B9c also impaired activation of ASK1 (Fig. 4c), a known upstream activator of p38 in neurons (Takeda et al., 2004) (as measured by analysing Thr-854 phosphorylation). Taken together, the data in Fig. 3 and Fig. 4a-c support the hypothesis that NMDAR-dependent activation of p38 can be triggered by submembranous Ca^{2+}, and requires the NR2 PDZ ligand to couple to associated proteins in cortical neurons.

Consistent with previous studies, TAT-NR2B9c reduced NMDAR-dependent neuronal death as assayed by studying nuclear pyknosis (Fig. 4d, example phase-contract pictures also shown). Using an alternative assay of cell viability, ATP levels, TAT-NR2B9c also reduced NMDAR-dependent neuronal death (Fig. 4e). We next investigated whether the neurons “protected” by TAT-NR2B9c were functional, focusing on the TAT-NR2B9c-treated neurons that were exposed to an ordinarily toxic dose of NMDA (40 μM). In current-clamp recordings, we injected current into the surviving cells (with 300 ms pulses at 1 Hz) to bring them to threshold. In current clamp configuration, all surviving cells studied fired action potential bursts when depolarized beyond −40 mV, as was observed with non-NMDA treated neurons (see examples in Fig. 4f). In voltage-clamp, we also measured spontaneous EPSC (sEPSC) frequency in surviving cells, to determine whether surviving neurons remained synaptically connected to other neurons. The prolonged nature of these sEPSCs presumably reflects the fact that these events are associated with action-potential bursts of activity that occur in the rest of the network of cultured neurons. In neurons treated with 40 μM NMDA alone there was a severe decrease in sEPSC frequency of surviving cells (Fig. 4g), consistent with the large amount of cell death (each surviving neuron would be connected to fewer neurons). In contrast, neurons that are protected by TAT-NR2B9c following an excitotoxic insult exhibit no such reduction in sEPSC frequency (Fig. 4g), indicating that not only does TAT-NR2B9c prevent cell death, but that by this assay, overall connectivity and excitability of the neurons are preserved.

TAT-NR2B9c reduces focal ischemic brain damage in rats (Aarts et al., 2002) and results above suggest that this may be via p38 inhibition. If this were the case, then the model of focal ischemia amenable to protection by TAT-NR2B9c (Aarts et al., 2002) should cause brain damage that is p38-dependent. We performed the 3 pial vessel (3PVO) model of focal ischemia on adult rats, which involves cauterization of three terminal pial branches of the middle cerebral artery. Brain injury following 3PVO is nearly completely protected by treatment with TAT-NR2B9c (Fig. 4h,i). We then tested the effect of administering the p38 inhibitor SB202190 and found that this too offered very strong protection against brain damage following 3PVO (Fig. 4h,i, Fig. S2) suggesting that TAT-NR2B9c and the p38 inhibitor may be acting on a common pathway *in vivo*, as is the case *in vitro*.

TAT-NR2B9c does not block survival or plasticity signaling, unlike conventional NMDAR antagonists

An aim of this study is to determine whether the NMDAR can be uncoupled from pro-death signaling without impairing pro-survival signaling, or synaptic plasticity. We first investigated the effect of TAT-NR2B9c on PI3K-Akt signaling and activation of CREB-dependent gene expression, key mediators of synaptic NMDAR-dependent neuroprotection (Papadia et al., 2005; Hardingham, 2006). TAT-NR2B9c did not impair activation of CREB-dependent reporter activation triggered by an episode of synaptic NMDAR activity lasting 1 h or 30 min (Fig. 5a and data not shown). In fact, TAT-NR2B9c had a small but significant potentiating effect (Fig. 5a), the basis for which is not clear. Consistent with an absence of a role for either p38 or JNK in activity-dependent CREB activation, neither SB203580 nor SP600125 impaired activation of the CRE reporter (data not shown). TAT-NR2B9c also did not interfere with activity-dependent induction of a CREB target gene *Adcyap1* (Fukuchi et al., 2005), which encodes the neuroprotective ligand Pituitary Adenylate Cyclase-Activating Polypeptide (PACAP, data not shown). TAT-NR2B9c had no effect on synaptic NMDAR signaling to Akt activation triggered by an episode of synaptic NMDAR activity lasting 1 h or 30 min (Fig. 5b and data not shown). The NMDAR antagonist MK-801 promotes apoptotic-like neurodegeneration in trophically deprived conditions (Papadia et al., 2005). However, TAT-NR2B9c did not promote neuronal death, in contrast to MK-801 (Fig. 5c).

We next sought to determine whether TAT-NR2B9c impaired NMDAR-dependent synaptic plasticity. We employed a neuronal culture model of plasticity (Arnold et al., 2005) in which a brief period of bicuculline-induced bursting causes an NMDAR-dependent increase in miniature excitatory postsynaptic current (mEPSC) frequency in hippocampal neurons (Fig. 5d, 5e for example traces), attributed to AMPA receptor insertion and unsilencing of synapses (Abegg et al., 2004). We found that, while MK-801 blocked the increase in mEPSC frequency, TAT-NR2B9c had no effect (Fig. 5d,e). SP600125 did not suppress the synaptic NMDAR-dependent enhancement of mEPSC frequency, however, SB203580 did have an inhibitory effect (data not shown). Thus, TAT-NR2B9c has a clear advantage over a global small molecule inhibitor of p38 with regard to unwanted interference with this plasticity model.

We also studied the effect of TAT-NR2B9c on basal activity and found that mEPSC frequency was not altered by TAT-NR2B9c, nor was sEPSC frequency affected (data not shown), indicating that overall excitability of the neuronal network is not altered. Thus, TAT-NR2B9c can impair NMDAR-dependent pro-death signaling, without interfering appreciably with NMDAR-dependent pro-survival signaling or a model of NMDAR-dependent synaptic plasticity.

JNK activation by mitochondrial ROS

The JNK-dependency of NMDAR-mediated cell death of NR-AtT20 cells revealed that this signaling cassette may not require the NMDAR signaling complex. Consistent with this, TAT-

NR2B9c did not interfere with JNK activation (Fig. 4b). These observations raise the possibility that the Ca^{2+} effector of JNK activation may be away from the NMDA receptor signaling complex at a different subcellular location. Ca^{2+} uptake into mitochondria, through the potential-driven uniporter, is known to play a role in NMDAR-dependent cell death (Stout et al., 1998) and triggers the production of reactive oxygen species (ROS) (Nicholls, 2004), regulators of JNK signaling (Torres and Forman, 2003). To investigate the role of mitochondrial ROS production in JNK activation, we treated neurons with the mitochondrially targeted ubiquinone-based antioxidant, MitoQ (Kelso et al., 2001). MitoQ strongly inhibited NMDA-induced JNK signaling, (Fig. 6a, but not p38 activation, Fig. 6b) while the targeting moiety (DTPP) had no effect on JNK (Fig. 6a). Recently, protein kinase D (PKD, also known as PKCμ) was shown to mediate the activation of JNK signaling by ROS in HEK cells (Eisenberg-Lerner and Kimchi, 2007). To investigate the role of PKCμ/PKD in neurons we employed the established method of applying PKC isoform inhibitors with slightly different specificities (Lemonnier et al., 2004;Zhang et al., 2005;Ivison et al., 2007): Go6976 inhibits multiple isoforms of PKC, including α, β and μ (PKD) isoforms, while Go6983 blocks PKCα, β, γ, δ and ζ isoforms, but not PKCμ/PKD. We found that Go6976, but not Go6983, inhibited NMDAR-dependent JNK signaling (Fig. S3). Since PKCμ/PKD is the only known kinase that is inhibited by Go6976 but not by Go6983, this implicates PKCμ/PKD in the activation of JNK by NMDAR-dependent mitochondrial ROS production. However, we cannot rule out that any hitherto unknown kinases that are blocked by Go6976, but not Go6983 could also be responsible for the effects that we observe.

An implication of the inhibitory effect of MitoQ is that interfering with mitochondrial Ca^{2+} uptake may impair JNK signaling. NMDAR activation induces a dose-dependent increase in vesicular Ca^{2+} load, the majority of which is mitochondrial (Ward et al., 2005). Mitochondrial Ca^{2+} uptake can be prevented by pre-depolarizing the mitochondria with the uncoupler FCCP, which has been reported to reduce NMDAR-dependent cell death (Stout et al., 1998). We treated neurons with FCCP plus the mitochondrial ATPase inhibitor oligomycin (to prevent depletion of cytoplasmic ATP through ATPase reversal). FCCP/oligomycin (F/O) pre-treatment dramatically reduced vesicular Ca^{2+} uptake triggered by 20 μM NMDA (Fig. 6c), confirming that most NMDA-induced vesicular Ca^{2+} uptake was into mitochondria (the remainder being into the ER (Ward et al., 2005)). Consistent with a major uptake mechanism being blocked, cytoplasmic Ca^{2+} load triggered by 20 μM NMDA was increased by F/O pretreatment (Fig. 6d) to levels similar to those induced by 50 μM NMDA in the absence of F/O. Indeed, F/O pretreatment inhibited NMDA-induced JNK signaling (Fig. 6e,f), whilst NMDAR coupling to p38 and ERK1/2 activation was not affected (Fig. 6g,h).

Effective anti-excitotoxic therapy by combining TAT-NR2B9c with a TAT-fused JNK inhibitor *in vitro* and *in vivo*

Interestingly, we found that TAT-NR2B9c was not neuroprotective at high doses of NMDA (100 μM, Fig. 7a). Given that TAT-NR2B9c interferes with NMDAR pro-death signaling to p38 and not JNK, we hypothesized that both pathways must be blocked to achieve protection following exposure to high doses of NMDA. We tested the neuroprotective effect of TAT-NR2B9c in combination with the cell-permeable peptide JNK inhibitor, D-JNKI1 (Borsello et al., 2003), (Fig. 2a). While either peptide alone was protective against moderate doses of NMDA, neither was effective against 100 μM NMDA. However, when combined they offered significant neuroprotection at 100 μM NMDA (Fig. 7a). Thus, both SAPK pathways must be blocked to offer neuroprotection against a severe excitotoxic insult. While both TAT-NR2B9c and D-JNKI1 protect against models of rodent focal ischemia (Aarts et al., 2002;Borsello et al., 2003), we hypothesized that they may work well in combination *in vivo*. Given the efficacy of these peptides on their own, we sought a severe model of ischemia beyond the protective effects of either peptide individually.

D-JNKI1 alone gives strong protection against focal ischemia due to middle cerebral artery occlusion (MCAO) in neonatal rats or adult mice (Borsello et al., 2003), so we created a stronger ischemic insult in P12 rats by combining MCAO with 90 min closure of the ipsilateral common carotid artery (MCAO+) (Renolleau et al., 1998). This produces more complete ischemia reducing irrigation of the ischemic zone by anastomoses from the anterior and posterior cerebral arteries. MCAO+ resulted in larger infarcts than MCAO (Fig. 7b). Furthermore, while D-JNKI1 alone given 6 h *after* the onset of ischemia reduced the infarct volume in the MCAO model (Fig. 7b, 7c for examples), the same dose given either 30 min before or 6 h after the MCAO+ procedure was ineffective (Fig. 7d). The effects of TAT-NR2B9c alone or in combination with D-JNKI1 were also tested. Since the therapeutic window for D-JNKI1 is 12 h (Borsello et al., 2003), we administered D-JNKI1 at 6 h after the onset of ischemia. TAT-NR2B9c was given 30 min before ischemia since the therapeutic window for its use was unknown. TAT-NR2B9c alone did not significantly reduce the volume of the infarct, but its combination with D-JNKI1 gave significant protection (Fig. 7e, 7f, Fig. S4). Therefore, inhibiting NMDAR pro-death signals that are both dependent on the NSC (p38) and independentof it (JNK) has synergistically protective effects in severe excitotoxic scenarios *in vitro* and *in vivo*.

Discussion

We show here that the NMDAR can be uncoupled from pro-death signaling without interfering in models of synaptic NMDAR-dependent neuroprotection and synaptic plasticity. We also demonstrate that NMDAR signaling to JNK and p38 has differing dependencies on neuron-specific signaling proteins and the NR2B PDZ ligand, yet both contribute to excitotoxic death. Targeting both pathways relies on separate approaches and provides effective protection from excitotoxicity *in vitro* and *in vivo*.

Failed clinical trials for stroke with NMDAR antagonists

Despite evidence from animal studies implicating the NMDAR in ischemic brain damage, clinical trials of NMDAR antagonists for stroke have failed due to poor tolerance and efficacy (Ikonomidou and Turski, 2002; Muir, 2006). The important role of NMDARs in the CNS may mean that for any antagonist, the maximal tolerated dose is lower than the therapeutically effective dose, since many unacceptable side-effects are on-target effects. Evidence that NMDAR activity can exert a neuroprotective effect has led to suggestions that it may even promote recovery post-reperfusion, and prevent delayed neuronal loss in the penumbra (Albers et al., 2001; Ikonomidou and Turski, 2002). As such, antagonists may be protective early in the insult but not later on, which indicates a potential need for more specific anti-excitotoxic strategies where the effects on pro-survival NMDAR signaling are considered.

NMDAR activated survival and death signals require spatially distinct pools of Ca^{2+}

Activation of CREB is an important mediator of synaptic NMDAR-dependent neuroprotection (Papadia et al., 2005). Elevation ofCa^{2+} within the nucleus is important for full activation of CREB-dependent gene expression and resultant neuroprotection (Hardingham et al., 1997; Hardingham et al., 2001b; Papadia et al., 2005), likely due to the nuclear localisation of CREB's activator CaMKIV. Nuclear Ca^{2+} is also implicated in regulating memory consolidation (Limback-Stokin et al., 2004), though whether this is via CREB activation is not known. Thus, the nucleus is a major site for physiological effects ofNMDAR signaling. However, it does not appear to play a role in excitotoxic cell death since inhibition of nuclear Ca^{2+}/calmodulin signaling does not interfere with NMDAR-dependent excitotoxic cell death (GEH, unpublished). Another key NMDAR-activated pro-survival signal, the PI3K-Akt pathway (Hetman and Kharebava, 2006), is likely to be activated by cytoplasmic Ca^{2+} elevation, due to the Ca^{2+}/calmodulin dependence of PI3K (Joyal et al., 1997). Our results support this since

submembranous Ca^{2+} is insufficient to trigger this pathway (Fig. 3d,f). On the other hand, submembranous Ca^{2+} transients are sufficient to activate p38 signaling (Fig. 3d,e), which is a Ca^{2+} pool not involved in either pro-survival pathway. In contrast, pro-death signaling via JNK may directly or indirectly involve Ca^{2+} uptake into mitochondria and mitochondrial ROS production (Fig. 6). Ca^{2+} uptake into mitochondria has been shown to trigger ROS production (Nicholls, 2004), suggesting that mitochondrial ROS generation, potentially triggered by mitochondrial Ca^{2+} uptake, is a trigger for JNK signaling. Thus in cortical neurons, the NMDAR activated effectors of survival and death have very different spatial requirements for Ca^{2+}.

Role of the NR2B PDZ ligand in death signaling

The cell-permeable TAT-based NR2B9c fusion peptide protects against excitotoxicity *in vitro* and *in vivo* by uncoupling NR2B from PSD-95 and downstream signaling molecules such as nNOS (Aarts et al., 2002) and p38 MAP kinase (this study). Moreover, a model of ischemia where TAT-NR2B9c is highly neuroprotective is also responsive to a p38 inhibitor (Fig. 4h,i), suggesting that TAT-NR2B9c acts *in vivo* by impairing pro-death p38 signaling. Despite its efficacy, TAT-NR2B9c would be of limited benefit over conventional NMDAR antagonists if it impaired physiological pro-survival and plasticity signaling. However, at therapeutic concentrations, TAT-NR2B9c did not interfere with neuronal culture models of these processes, nor did it affect basal network activity. The fact that TAT-NR2B9c did not impair Ca^{2+} influx nor affect our model of NMDAR-dependent synaptic plasticity suggests that interactions with the NR2B PDZ ligand may be dispensable for plasticity at least in the short term (although effects on other models of plasticity cannot be ruled out).

While global NMDAR blockade is not thought to be a viable therapeutic option, a specific role for NR2B-NMDARs in promoting cell death has been suggested (Liu et al., 2007) and would enable this particular subtype of NMDAR to be targeted without impairing pro-survival signaling, using the highly selective antagonists available. However, we recently found that NR2B-NMDARs are capable of promoting both survival and death signaling (Martel et al., 2008). Interestingly, NMDARs have been reported to mediate p38 *de*phosphorylation in hippocampal neurons (Krapivinsky et al., 2004; Waxman and Lynch, 2005) mediated by NR2B-NMDARs (Waxman and Lynch, 2005), which is presumably a protective response that NR2B antagonists would block. Moreover, NR2A-NMDARs were recently shown to be capable of mediating excitotoxicity as well as protective signaling (von Engelhardt et al., 2007). Taken together, these studies indicate that NR2B-NMDARs and NR2A-NMDARs are both capable of mediating survival and death signaling. Thus, the specific ability of NR2B-NMDARs and NR2A-NMDARs to promote death and survival respectively (Liu et al., 2007) may not apply in all neuronal types at all developmental stages.

The inability of TAT-NR2B9c to uncouple the NMDAR from JNK signaling (Fig. 4b) or impair JNK-mediated, NMDAR-dependent death of NR-AtT20 cells (data not shown) indicates that the JNK pathway does not rely heavily on the NR2B PDZ domain. This is consistent with mitochondrial ROS production being the trigger for this pro-death signal, rather than membrane-proximal events. Our data implicate PKD as a potential NMDAR-induced activator of JNK signaling by NMDAR activation (Fig. S3). ROS can induce JNK signaling in HEK293 cells by activating Death-associated protein kinase (DAPK), which in turn activates PKD (Eisenberg-Lerner and Kimchi, 2007). The role of DAPK in JNK activation in our model awaits investigation, but interestingly DAPK has been found to contribute to cerebral ischemic injury (Shamloo et al., 2005).

The neuroprotective effects of uncoupling NR2B from PSD-95 provide a convincing explanation for the observation that Ca^{2+} influx specifically through NMDARs promotes cell death: i.e. that Ca^{2+}-dependent cell death is “source specific” (Tymianski et al., 1993).

However, this model is not universally accepted: the idea that simply a high Ca^{2+} load is the main reason for NMDAR-dependent cell death is supported by the fact that cell death can be reconstituted in non-neuronal cells by expressing NMDARs in the absence of their associated signaling complexes (Cik et al., 1993). Our data suggest that both models are partially correct: efficient p38 signaling requires the NMDAR signaling complex and could be viewed as source-specific, while JNK signaling does not. We did not examine calpain activation in this study: while NMDAR activity is a typical physiological activator of calpains in neurons, it is unclear whether this is due to the high Ca^{2+} load triggered or due to specific coupling via structural molecules. Interestingly, a precedent for the latter exists in the case of Focal Adhesion Kinase, which recruits both calpain and ERK, resulting in ERK-mediated phosphorylation and activation of calpain (Wells et al., 2005).

Ca^{2+} influx dependent on intense synaptic NMDAR activation is well tolerated by hippocampal neurons whereas activation of extrasynaptic NMDARs, either on their own or in the presence of synaptic NMDAR activation, causes a loss of mitochondrial membrane potential and cell death (Hardingham et al., 2002). These findings have been recapitulated by others in cortical neurons (Leveille et al., 2005), raising the possibility that this is a general CNS phenomenon. At first glance these observations are at apparent odds with the protecting effects of TAT-NR2B9c, if we assume that TAT-NR2B9c exerts its effect by uncoupling synaptic NMDARs from PSD-95 and nNOS activation. However, TAT-NR2B9c could conceivably be exerting its effects on extrasynaptic as well as synaptic NMDARs. While immunohistochemical studies show PSD-95 to be mostly in synaptic puncta, this does not rule out a more diffuse distribution of PSD-95 at extrasynaptic sites, interacting with extrasynaptic NMDARs. Moreover, extrasynaptic clusters of PSD-95 have been observed in hippocampal neurons at a frequency of almost half that of synaptic clusters (Carpenter-Hyland and Chandler, 2006). Another possibility is that extrasynaptic NR2 PDZ ligands form interactions with a death effector other than PSD-95, which are also disrupted by TAT-NR2B9c.

Even if TAT-NR2B9c is acting specifically on synaptic NMDARs, it could be that synaptic NMDAR signaling to p38 contributes to cell death in the context of a neuron experiencing chronic extrasynaptic NMDAR activity. There is a good deal of evidence implicating p38 as a mediator of NMDAR-dependent excitotoxicity (Kawasaki et al., 1997; Cao et al., 2004; Rivera-Cervantes et al., 2004; Molz et al., 2007). However, non-toxic episodes of NMDAR activity (e.g. induced by bicuculline, or low doses of NMDA) can also activate p38, indicating that p38 only contributes to toxicity in certain contexts. Thus, it is possible that synaptic NMDAR signaling to p38 is tolerated during an episode of synaptic activity, however, it may be harmful when induced in a cell under stress from chronically elevated levels of extracellular glutamate (e.g. following an ischemic episode).

Another intriguing question surrounding the action of TAT-NR2B9c is whether it is acting via pathways other than simply inhibiting p38 activation. This seems likely, since the protective effect of TAT-NR2B9c is at least as good as that of p38 inhibitors, despite not completely inhibiting p38 activation by NMDA. Other pro-death pathways may be inhibited, for example other toxic actions of NO production. Alternatively, a lack of protein interactions at the NR2 PDZ ligand may facilitate the binding of other signaling molecules that promote a pro-survival effect.

Future therapy combinations in stroke trials?

Therapies that target downstream death pathways in combination may be effective in blocking NMDAR pro-death signaling, such as a combination of TAT-NR2B9c and DJNKI, both of which are effective if administered after the commencement of ischemia (Aarts et al., 2002; Borsello et al., 2003). While in our model, the SAPKs p38 and JNK are the main mediators of excitotoxicity, other mediators of ischemic cell death include calpain-dependent cleavage of

the Na^+/Ca^{2+} exchanger (Bano et al., 2005), and activation of TRPM7 channels (Aarts et al., 2003). The precise pathway(s) that mediate ischemic brain damage may depend on the neuronal subtype, the severity and duration of the episode, and the position of the neuron within the ischemic zone (core or penumbra). Therefore, it may be that additional molecules that target calpain or TRPM7 activation may be yet more effective as part of a cocktail of anti-death signaling drugs. Their use, where appropriate, in conjunction with the thrombolytic drug tPA may aid in rapid drug delivery to the site of insult.

Supplementary Material

Refer to Web version on PubMed Central for supplementary material.

Acknowledgements

We thank Christophe Bonny for D-JNKI1, Mike Murphy for MitoQ and Hidenori Ichijo and Anne Stephenson for plasmids, Rudolf Kraftsik for help with statistics and Sonia Naegele for technical assistance. Supported by the EC FP6 STRESSPROTECT (LHSM-CT-2004-005310), The Wellcome Trust, BBSRC, and grant 7057.2 BTS-LS from the Swiss CTI/KTI and the Network of European Neuroscience Institutes. G.E.H is supported by a Royal Society University Research Fellowship.

References

Aarts M, Iihara K, Wei WL, Xiong ZG, Arundine M, Cerwinski W, MacDonald JF, Tymianski M. A key role for TRPM7 channels in anoxic neuronal death. Cell 2003;115:863–877. [PubMed: 14697204]

Aarts M, Liu Y, Liu L, Besshoh S, Arundine M, Gurd JW, Wang YT, Salter MW, Tymianski M. Treatment of ischemic brain damage by perturbing NMDA receptor- PSD-95 protein interactions. Science 2002;298:846–850. [PubMed: 12399596]

Abegg MH, Savic N, Ehrengruber MU, McKinney RA, Gahwiler BH. Epileptiform activity in rat hippocampus strengthens excitatory synapses. J Physiol 2004;554:439–448. [PubMed: 14594985]

Adams SM, de Rivero Vaccari JC, Corriveau RA. Pronounced cell death in the absence of NMDA receptors in the developing somatosensory thalamus. J Neurosci 2004;24:9441–9450. [PubMed: 15496680]

Albers GW, Goldstein LB, Hall D, Lesko LM. Aptiganel hydrochloride in acute ischemic stroke: a randomized controlled trial. Jama 2001;286:2673–2682. [PubMed: 11730442]

Anegawa NJ, Guttmann RP, Grant ER, Anand R, Lindstrom J, Lynch DR. N-Methyl-D-aspartate receptor mediated toxicity in nonneuronal cell lines: characterization using fluorescent measures of cell viability and reactive oxygen species production. Brain Res Mol Brain Res 2000;77:163–175. [PubMed: 10837912]

Arnold FJ, Hofmann F, Bengtson CP, Wittmann M, Vanhoutte P, Bading H. Microelectrode array recordings of cultured hippocampal networks reveal a simple model for transcription and protein synthesis-dependent plasticity. J Physiol 2005;564:3–19. [PubMed: 15618268]

Arundine M, Tymianski M. Molecular mechanisms of glutamate-dependent neurodegeneration in ischemia and traumatic brain injury. Cell Mol Life Sci 2004;61:657–668. [PubMed: 15052409]

Bading H, Greenberg ME. Stimulation of protein tyrosine phosphorylation by NMDA receptor activation. Science 1991;253:912–914. [PubMed: 1715095]

Bading H, Ginty DD, Greenberg ME. Regulation of gene expression in hippocampal neurons by distinct calcium signaling pathways. Science 1993;260:181–186. [PubMed: 8097060]

Bano D, Young KW, Guerin CJ, Lefeuvre R, Rothwell NJ, Naldini L, Rizzuto R, Carafoli E, Nicotera P. Cleavage of the plasma membrane Na+/Ca2+ exchanger in excitotoxicity. Cell 2005;120:275–285. [PubMed: 15680332]

Baxter AW, Wyllie DJ. Phosphatidylinositol 3 kinase activation and AMPA receptor subunit trafficking underlie the potentiation of miniature EPSC amplitudes triggered by the activation of L-type calcium channels. J Neurosci 2006;26:5456–5469. [PubMed: 16707798]

Boeckman FA, Aizenman E. Pharmacological properties of acquired excitotoxicity in Chinese hamster ovary cells transfected with N-methyl-D-aspartate receptor subunits. J Pharmacol Exp Ther 1996;279:515–523. [PubMed: 8930153]

Borsello T, Clarke PG, Hirt L, Vercelli A, Repici M, Schorderet DF, Bogousslavsky J, Bonny C. A peptide inhibitor of c-Jun N-terminal kinase protects against excitotoxicity and cerebral ischemia. Nat Med 2003;9:1180–1186. [PubMed: 12937412]

Camacho A, Massieu L. Role of glutamate transporters in the clearance and release of glutamate during ischemia and its relation to neuronal death. Arch Med Res 2006;37:11–18. [PubMed: 16314180]

Cao J, Semenova MM, Solovyan VT, Han J, Coffey ET, Courtney MJ. Distinct requirements for p38alpha and c-Jun N-terminal kinase stress-activated protein kinases in different forms of apoptotic neuronal death. J Biol Chem 2004;279:35903–35913. [PubMed: 15192112]

Cao J, Viholainen JI, Dart C, Warwick HK, Leyland ML, Courtney MJ. The PSD95-nNOS interface: a target for inhibition of excitotoxic p38 stress-activated protein kinase activation and cell death. J Cell Biol 2005;168:117–126. [PubMed: 15631993]

Carpenter-Hyland EP, Chandler LJ. Homeostatic plasticity during alcohol exposure promotes enlargement of dendritic spines. Eur J Neurosci 2006;24:3496–3506. [PubMed: 17229098]

Chohan MO, Iqbal K. From tau to toxicity: Emerging roles of NMDA receptor in Alzheimer's disease. J Alzheimers Dis 2006;10:81–87. [PubMed: 16988485]

Cik M, Chazot PL, Stephenson FA. Optimal expression of cloned NMDAR1/NMDAR2A heteromeric glutamate receptors: a biochemical characterization. Biochem J 1993;296(Pt 3):877–883. [PubMed: 7904155]

Coffey ET, Smiciene G, Hongisto V, Cao J, Brecht S, Herdegen T, Courtney MJ. c-Jun N-terminal protein kinase (JNK) 2/3 is specifically activated by stress, mediating c-Jun activation, in the presence of constitutive JNK1 activity in cerebellar neurons. J Neurosci 2002;22:4335–4345. [PubMed: 12040039]

Cui H, Hayashi A, Sun HS, Belmares MP, Cobey C, Phan T, Schweizer J, Salter MW, Wang YT, Tasker RA, Garman D, Rabinowitz J, Lu PS, Tymianski M. PDZ protein interactions underlying NMDA receptor-mediated excitotoxicity and neuroprotection by PSD-95 inhibitors. J Neurosci 2007;27:9901–9915. [PubMed: 17855605]

Eisenberg-Lerner A, Kimchi A. DAP kinase regulates JNK signaling by binding and activating protein kinase D under oxidative stress. Cell Death Differ 2007;14:1908–1915. [PubMed: 17703233]

Fujikawa DG, Shinmei SS, Cai B. Kainic acid-induced seizures produce necrotic, not apoptotic, neurons with internucleosomal DNA cleavage: implications for programmed cell death mechanisms. Neuroscience 2000;98:41–53. [PubMed: 10858610]

Fukuchi M, Tabuchi A, Tsuda M. Transcriptional regulation of neuronal genes and its effect on neural functions: cumulative mRNA expression of PACAP and BDNF genes controlled by calcium and cAMP signals in neurons. J Pharmacol Sci 2005;98:212–218. [PubMed: 16006741]

Ghatan S, Larner S, Kinoshita Y, Hetman M, Patel L, Xia Z, Youle RJ, Morrison RS. p38 MAP kinase mediates bax translocation in nitric oxide-induced apoptosis in neurons. J Cell Biol 2000;150:335–347. [PubMed: 10908576]

Gould E, Cameron HA, McEwen BS. Blockade of NMDA receptors increases cell death and birth in the developing rat dentate gyrus. Journal of Comparitive Neurology 1994;340:551–565.

Hardingham GE. Pro-survival signalling from the NMDA receptor. Biochem Soc Trans 2006;34:936–938. [PubMed: 17052231]

Hardingham GE, Bading H. The Yin and Yang of NMDA receptor signalling. Trends Neurosci 2003;26:81–89. [PubMed: 12536131]

Hardingham GE, Arnold FJ, Bading H. A calcium microdomain near NMDA receptors: on switch for ERK-dependent synapse-to-nucleus communication. Nat Neurosci 2001a;4:565–566. [PubMed: 11369935]

Hardingham GE, Arnold FJ, Bading H. Nuclear calcium signaling controls CREB-mediated gene expression triggered by synaptic activity. Nat Neurosci 2001b;4:261–267. [PubMed: 11224542]

Hardingham GE, Fukunaga Y, Bading H. Extrasynaptic NMDARs oppose synaptic NMDARs by triggering CREB shut-off and cell death pathways. Nat Neurosci 2002;5:405–414. [PubMed: 11953750]

Hardingham GE, Chawla S, Johnson CM, Bading H. Distinct functions of nuclear and cytoplasmic calcium in the control of gene expression. Nature 1997;385:260–265. [PubMed: 9000075]

Hetman M, Kharebava G. Survival signaling pathways activated by NMDA receptors. Curr Top Med Chem 2006;6:787–799. [PubMed: 16719817]

Ikonomidou C, Turski L. Why did NMDA receptor antagonists fail clinical trials for stroke and traumatic brain injury? The Lancet Neurology 2002;1:383–386.

Ikonomidou C, Stefovska V, Turski L. Neuronal death enhanced by *N*-methyl-D-aspartate antagonists. Proc Natl Acad Sci U S A 2000;97:12885–12890. [PubMed: 11058158]

Ikonomidou C, Bosch F, Miksa M, Bittigau P, Vockler J, Dikranian K, Tenkova TI, Stefovska V, Turski L, Olney JW. Blockade of NMDA receptors and apoptotic neurodegeneration in the developing brain. Science 1999;283:70–74. [PubMed: 9872743]

Ivison SM, Graham NR, Bernales CQ, Kifayet A, Ng N, Shobab LA, Steiner TS. Protein kinase D interaction with TLR5 is required for inflammatory signaling in response to bacterial flagellin. J Immunol 2007;178:5735–5743. [PubMed: 17442957]

Joyal JL, Burks DJ, Pons S, Matter WF, Vlahos CJ, White MF, Sacks DB. Calmodulin activates phosphatidylinositol 3-kinase. J Biol Chem 1997;272:28183–28186. [PubMed: 9353264]

Kawasaki H, Morooka T, Shimohama S, Kimura J, Hirano T, Gotoh Y, Nishida E. Activation and involvement of p38 mitogen-activated protein kinase in glutamate-induced apoptosis in rat cerebellar granule cells. J Biol Chem 1997;272:18518–18521. [PubMed: 9228012]

Kelso GF, Porteous CM, Coulter CV, Hughes G, Porteous WK, Ledgerwood EC, Smith RA, Murphy MP. Selective targeting of a redox-active ubiquinone to mitochondria within cells: antioxidant and antiapoptotic properties. J Biol Chem 2001;276:4588–4596. [PubMed: 11092892]

Krapivinsky G, Medina I, Krapivinsky L, Gapon S, Clapham DE. SynGAP-MUPP1-CaMKII synaptic complexes regulate p38 MAP kinase activity and NMDA receptor-dependent synaptic AMPA receptor potentiation. Neuron 2004;43:563–574. [PubMed: 15312654]

Lemonnier J, Ghayor C, Guicheux J, Caverzasio J. Protein kinase C-independent activation of protein kinase D is involved in BMP-2-induced activation of stress mitogen-activated protein kinases JNK and p38 and osteoblastic cell differentiation. J Biol Chem 2004;279:259–264. [PubMed: 14573624]

Leveille, F.; Nicole, O.; Buisson, A. Abstract Viewer/Itinerary Planner. Society for Neuroscience; Washington, DC: 2005. Cellular location of NMDA receptors influences their implication in excitotoxic injury. 2005 Online Program No. 946.2

Limback-Stokin K, Korzus E, Nagaoka-Yasuda R, Mayford M. Nuclear calcium/calmodulin regulates memory consolidation. J Neurosci 2004;24:10858–10867. [PubMed: 15574736]

Liu Y, Wong TP, Aarts M, Rooyakkers A, Liu L, Lai TW, Wu DC, Lu J, Tymianski M, Craig AM, Wang YT. NMDA receptor subunits have differential roles in mediating excitotoxic neuronal death both in vitro and in vivo. J Neurosci 2007;27:2846–2857. [PubMed: 17360906]

Martel M, Wyllie DJ, Hardingham GE. In developing hippocampal neurons, NR2B-containing NMDA receptors can mediate signalling to neuronal survival and synaptic potentiation, as well as neuronal death. Neuroscience. 2008doi:10.1016/j.neuroscience.2008.01.080

Mckenzie GJ, Stephenson P, Ward G, Papadia S, Bading H, Chawla S, Privalsky M, Hardingham GE. Nuclear Ca2+ and CaM kinase IV specify hormonal- and Notch-responsiveness. J Neurochem 2005;93:171–185. [PubMed: 15773917]

Molz S, Decker H, Dal-Cim T, Cremonez C, Cordova FM, Leal RB, Tasca CI. Glutamate-induced Toxicity in Hippocampal Slices Involves Apoptotic Features and p38(MAPK) Signaling. Neurochem Res. 2007

Muir KW. Glutamate-based therapeutic approaches: clinical trials with NMDA antagonists. Curr Opin Pharmacol 2006;6:53–60. [PubMed: 16359918]

Nicholls DG. Mitochondrial dysfunction and glutamate excitotoxicity studied in primary neuronal cultures. Curr Mol Med 2004;4:149–177. [PubMed: 15032711]

Olney JW. Brain lesions, obesity, and other disturbances in mice treated with monosodium glutamate. Science 1969;164:719–721. [PubMed: 5778021]

Papadia S, Hardingham GE. The Dichotomy of NMDA Receptor Signaling. Neuroscientist. 2007

Papadia S, Stevenson P, Hardingham NR, Bading H, Hardingham GE. Nuclear Ca2+ and the cAMP response element-binding protein family mediate a late phase of activity-dependent neuroprotection. J Neurosci 2005;25:4279–4287. [PubMed: 15858054]

Papadia S, Soriano FX, Leveille F, Martel MA, Dakin KA, Hansen HH, Kaindl A, Sifringer M, Fowler J, Stefovska V, McKenzie G, Craigon M, Corriveau R, Ghazal P, Horsburgh K, Yankner BA, Wyllie DJ, Ikonomidou C, Hardingham GE. Synaptic NMDA receptor activity boosts intrinsic antioxidant defenses. Nat Neurosci 2008;11:476–487. [PubMed: 18344994]

Renolleau S, Aggoun-Zouaoui D, Ben-Ari Y, Charriaut-Marlangue C. A model of transient unilateral focal ischemia with reperfusion in the P7 neonatal rat: morphological changes indicative of apoptosis. Stroke 1998;29:1454–1460. [PubMed: 9660403]discussion 1461

Rivera-Cervantes MC, Torres JS, Feria-Velasco A, Armendariz-Borunda J, Beas-Zarate C. NMDA and AMPA receptor expression and cortical neuronal death are associated with p38 in glutamate-induced excitotoxicity in vivo. J Neurosci Res 2004;76:678–687. [PubMed: 15139026]

Rutter AR, Stephenson FA. Coexpression of postsynaptic density-95 protein with NMDA receptors results in enhanced receptor expression together with a decreased sensitivity to L-glutamate. J Neurochem 2000;75:2501–2510. [PubMed: 11080203]

Shamloo M, Soriano L, Wieloch T, Nikolich K, Urfer R, Oksenberg D. Death-associated protein kinase is activated by dephosphorylation in response to cerebral ischemia. J Biol Chem 2005;280:42290–42299. [PubMed: 16204252]

Stout AK, Raphael HM, Kanterewicz BI, Klann E, Reynolds IJ. Glutamate-induced neuron death requires mitochondrial calcium uptake. Nat Neurosci 1998;1:366–373. [PubMed: 10196525]

Takeda K, Matsuzawa A, Nishitoh H, Tobiume K, Kishida S, Ninomiya-Tsuji J, Matsumoto K, Ichijo H. Involvement of ASK1 in Ca2+-induced p38 MAP kinase activation. EMBO Rep 2004;5:161–166. [PubMed: 14749717]

Tashiro A, Sandler VM, Toni N, Zhao C, Gage FH. NMDA-receptor-mediated, cell-specific integration of new neurons in adult dentate gyrus. Nature 2006;442:929–933. [PubMed: 16906136]

Torres M, Forman HJ. Redox signaling and the MAP kinase pathways. Biofactors 2003;17:287–296. [PubMed: 12897450]

Tovar KR, Westbrook GL. The incorporation of NMDA receptors with a distinct subunit composition at nascent hippocampal synapses *in vitro*. The Journal of Neuroscience 1999;19:4180–4188. [PubMed: 10234045]

Tymianski M, Charlton MP, Carlen PL, Tator CH. Source specificity of earlly calcium neurotoxicity in cultures embryonic spinal neurons. Journal of Neuroscience 1993;13:2085–2104. [PubMed: 8097530]

von Engelhardt J, Coserea I, Pawlak V, Fuchs EC, Kohr G, Seeburg PH, Monyer H. Excitotoxicity in vitro by NR2A- and NR2B-containing NMDA receptors. Neuropharmacology 2007;53:10–17. [PubMed: 17570444]

Ward MW, Kushnareva Y, Greenwood S, Connolly CN. Cellular and subcellular calcium accumulation during glutamate-induced injury in cerebellar granule neurons. J Neurochem 2005;92:1081–1090. [PubMed: 15715659]

Waxman EA, Lynch DR. N-methyl-D-aspartate receptor subtype mediated bidirectional control of p38 mitogen-activated protein kinase. J Biol Chem 2005;280:29322–29333. [PubMed: 15967799]

Wells A, Huttenlocher A, Lauffenburger DA. Calpain proteases in cell adhesion and motility. Int Rev Cytol 2005;245:1–16. [PubMed: 16125543]

Zhang SJ, Steijaert MN, Lau D, Schutz G, Delucinge-Vivier C, Descombes P, Bading H. Decoding NMDA Receptor Signaling: Identification of Genomic Programs Specifying Neuronal Survival and Death. Neuron 2007;53:549–562. [PubMed: 17296556]

Zhang W, Zheng S, Storz P, Min W. Protein kinase D specifically mediates apoptosis signal-regulating kinase 1-JNK signaling induced by H2O2 but not tumor necrosis factor. J Biol Chem 2005;280:19036–19044. [PubMed: 15755722]

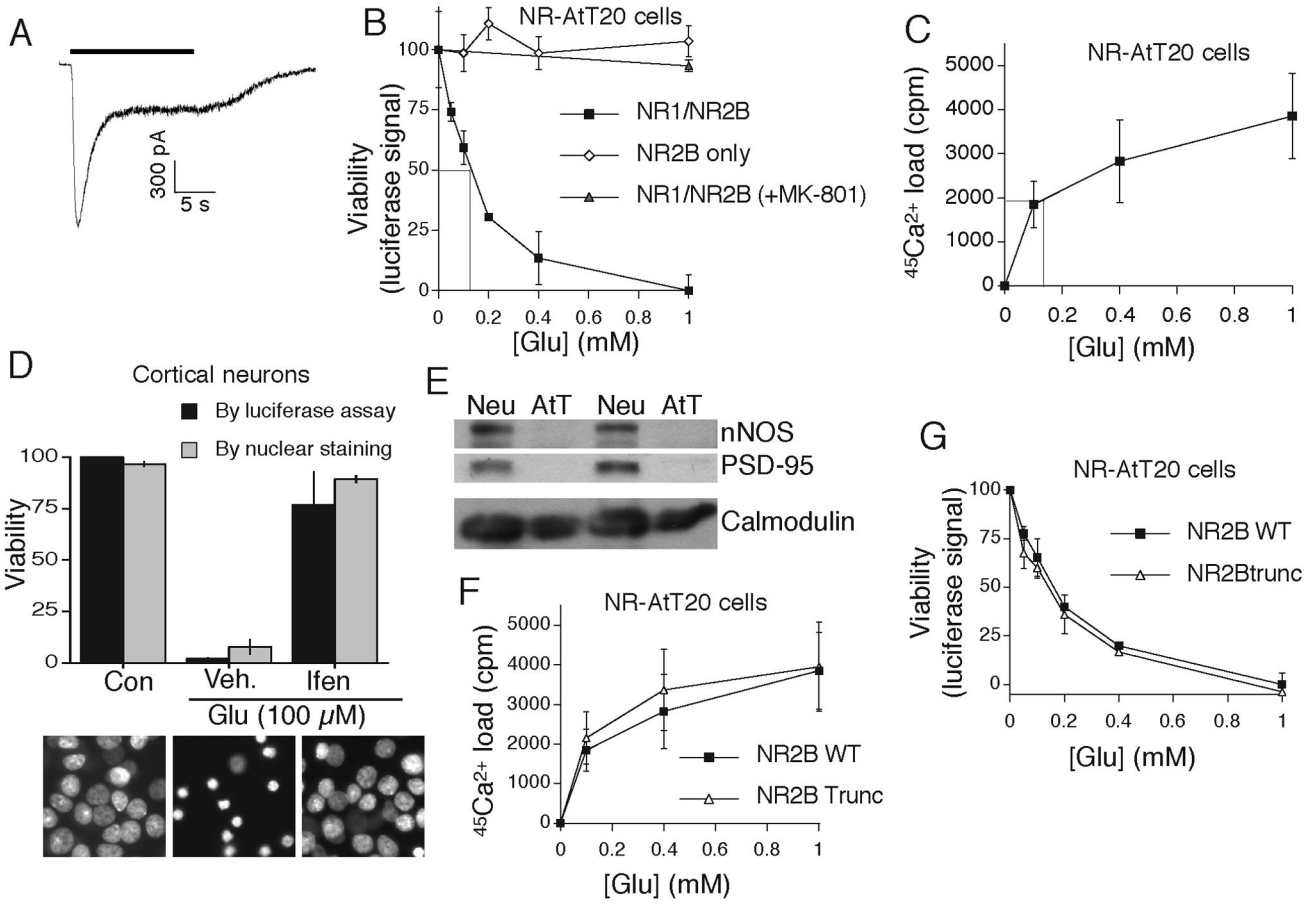

Fig. 1. NMDAR-mediated Ca^{2+} influx can kill NMDAR-expressing AtT20 cells in the absence of PSD-95, nNOS or the NR2 PDZ ligand

A) AtT20 cells transfected with pNR1 and pNR2B plasmids express functional NMDARs. Example trace of agonist (100 μM glutamate)-induced current in NMDAR-expressing AtT20 cells (NR-AtT20). B) Reconstituting NMDAR-dependent cell death in AtT20 cells. NR-AtT20 cells treated with glutamate for 5-7 h. Cells were co-transfected with pSV40-Luc to enable viability to be measured by performing a luciferase assay on lysates. *Mean ± s.e.m. shown in this and all subsequent Figs* (*n* =7). C) Measuring Ca^{2+} influx in NR-AtT20 cells. NR-AtT20 cells were incubated in $^{45}Ca^{2+}$-containing medium and treated with glutamate for 10 min (*n* =3). D) NR2B-containing NMDARs mediate excitotoxicity in DIV9 cortical neurons. Neurons treated as indicated with glutamate ± ifenprodil (3 μM). Neurons were transfected with pSV40-Luc to enable viability to be measured by a luciferase assay. In parallel, cell death was measured by counting pyknotic and non-pyknotic nuclei (*n* =3). Example pictures are shown (lower). E) Western analysis of nNOS and PSD-95 expression in equal quantities of protein extracts (by BCA assay) from AtT20 cells and cortical neurons. Calmodulin expression is also shown for comparison. F) NMDARs containing a truncated NR2B (lacking the C-terminal 4aa) mediate the same glutamate-dependent Ca^{2+} load as wild-type NR2B-containing NMDARs. AtT20 cells were transfected with pNR1 and either WT NR2B or NR2Btrunc. 24 h later cells were incubated in $^{45}Ca^{2+}$-containing medium and treated with glutamate for 10 min (*n* =3). G) NMDARs containing NR2Btrunc are equally effective at promoting glutamate-dependent cell death as wild-type NR2B-containing NMDARs. AtT20 cells were transfected with pNR1 and

either WT NR2B or NR2Btrunc, plus pSV40-Luc. 24 h post-transfection cells were treated with glutamate for 5-7 h prior to luciferase assay (n =3).

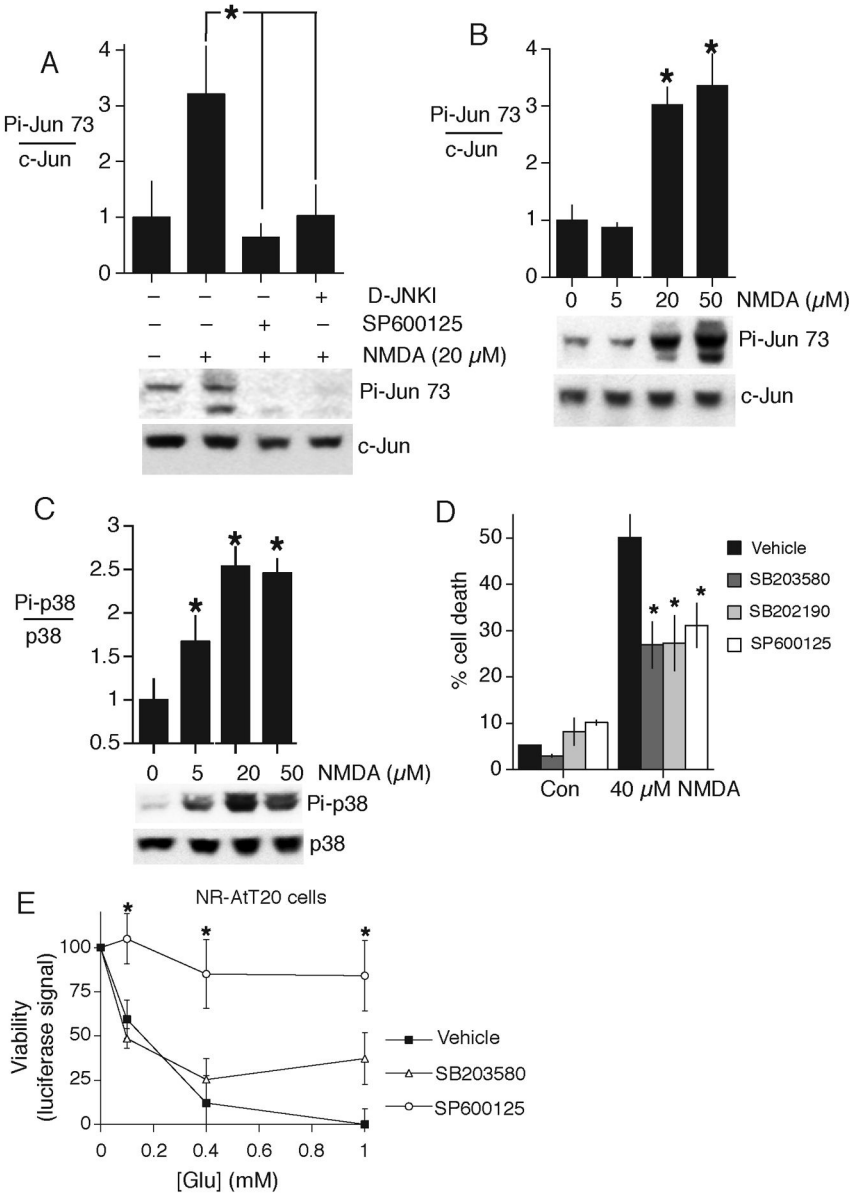

Fig. 2. Differing p38 MAPK dependency of NMDAR pro-death signaling in neurons vs. NR-AtT20 cells

A) NMDAR-dependent c-Jun phosphorylation is JNK-dependent. Cortical neurons treated with the JNK inhibitors SP600125 (3 μM) and DJNKI (2 μM) for 1 h prior to stimulation with NMDA (20 μM) for 30 min, $n = 3$. * $p < 0.05$, *2-tailed student's t-test in this and all subsequent figures unless indicated.* Western analysis of phospho-Jun (Ser73) levels were normalized to c-Jun levels ($n = 3$). B) Western analysis of the dose response of JNK-dependent Jun phosphorylation with NMDA stimulation in cortical neurons ($n = 5$). C) Western analysis of the dose response of p38 phosphorylation with NMDA stimulation in cortical neurons ($n = 5$). D) NMDAR-mediated neuronal cell death is mediated by both JNK and p38 signaling. Neurons treated with inhibitors of p38 (SB203580, 5μM, SB202190, 5μM) or JNK (SP600125, 1 μM) for 1 h prior to a 1 h excitotoxic insult. Neuronal loss was assessed after 24 h ($n = 3$). E) NMDAR-dependent death of NR-AtT20 cells is totally JNK-dependent. NR-AtT20 cells treated with inhibitors of p38 (SB203580) or JNK (SP600125) for 1 h prior to glutamate

treatment at the indicated concentrations. Luciferase assay performed 5-7 h later. *p <0.05 indicates significant protection compared to control (n =3).

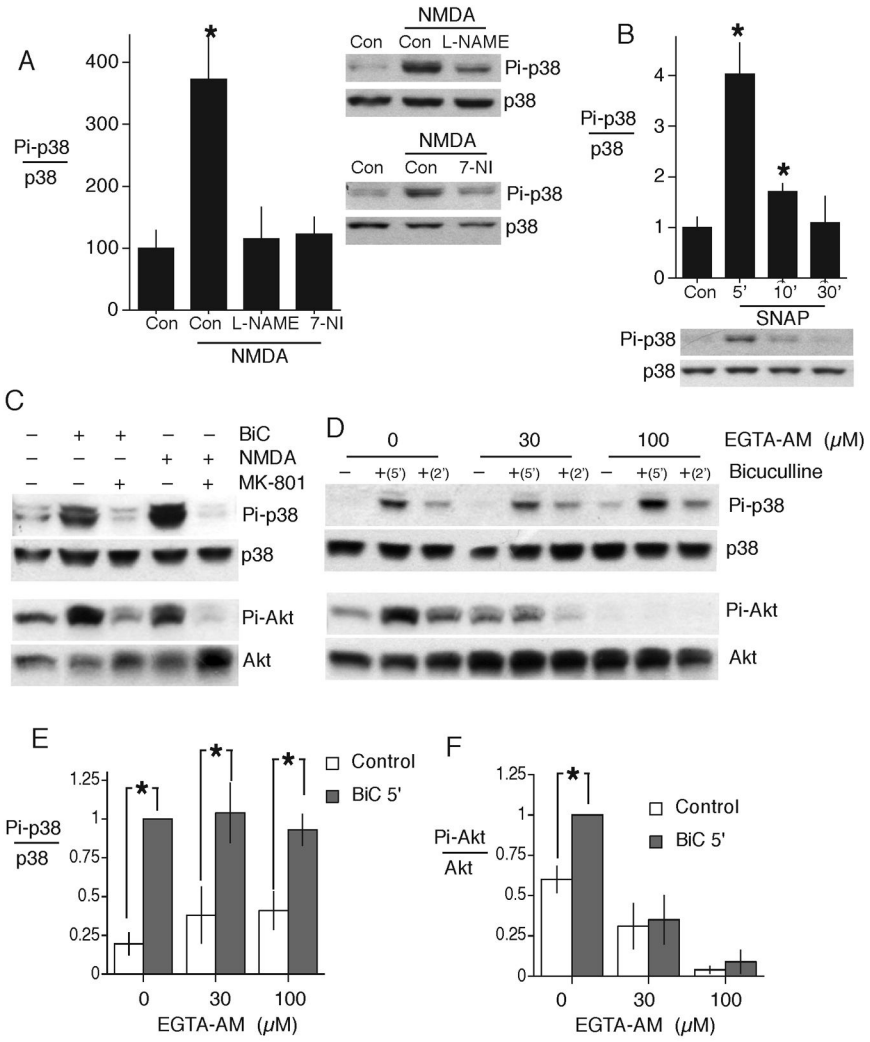

Fig. 3. NMDAR signaling to p38 MAPK in cortical neurons involves NOS and requires only submembranous Ca^{2+}

A) NMDAR-dependent p38 activation in cortical neurons is NOS-dependent. Neurons were placed in arginine-free medium and treated with either vehicle or a NOS inhibitor for 1 h (L-NAME at 500 μM and 7-Nitroindazole at 5 μM). Neurons were then stimulated with NMDA (20 μM) for 5 min prior to harvesting and Western analysis (n =4). B) Nitric Oxide donor SNAP is sufficient to induce p38 activation in cortical neurons. Neurons were treated with the NO donor S-Nitroso-N- acetylpenicillamine (SNAP, 500 μM) for the indicated times prior to harvesting and Western analysis (p <0.05 compared to untreated neurons, n =3-4). C) Bicuculline-induced synaptic activity promotes NMDAR-dependent p38 and Akt activation. Western analysis of p38 and Akt activation in cortical neurons using phospho-specific antibodies. Neurons stimulated with NMDA (20 μM) or bicuculline (BiC, 50 μM) for 5 min ± MK-801 (10 μM). D-F) Eliminating global Ca^{2+} transient by loading neurons with EGTA-AM does not affect p38 activation, but abolishes Akt activation. D) Western analysis of p38 and Akt activation in neurons stimulated with bicuculline for 2 or 5 min. Prior to bicuculline stimulation, neurons were pre-loaded with EGTA-AM at room temperature for 20 min (Hardingham et al., 2001a). E) Analysis of the effect of EGTA-AM on bicuculline-induced p38 activation (n =3). F) Analysis of the effect of EGTA-AM on bicuculline-induced Akt activation (n =3).

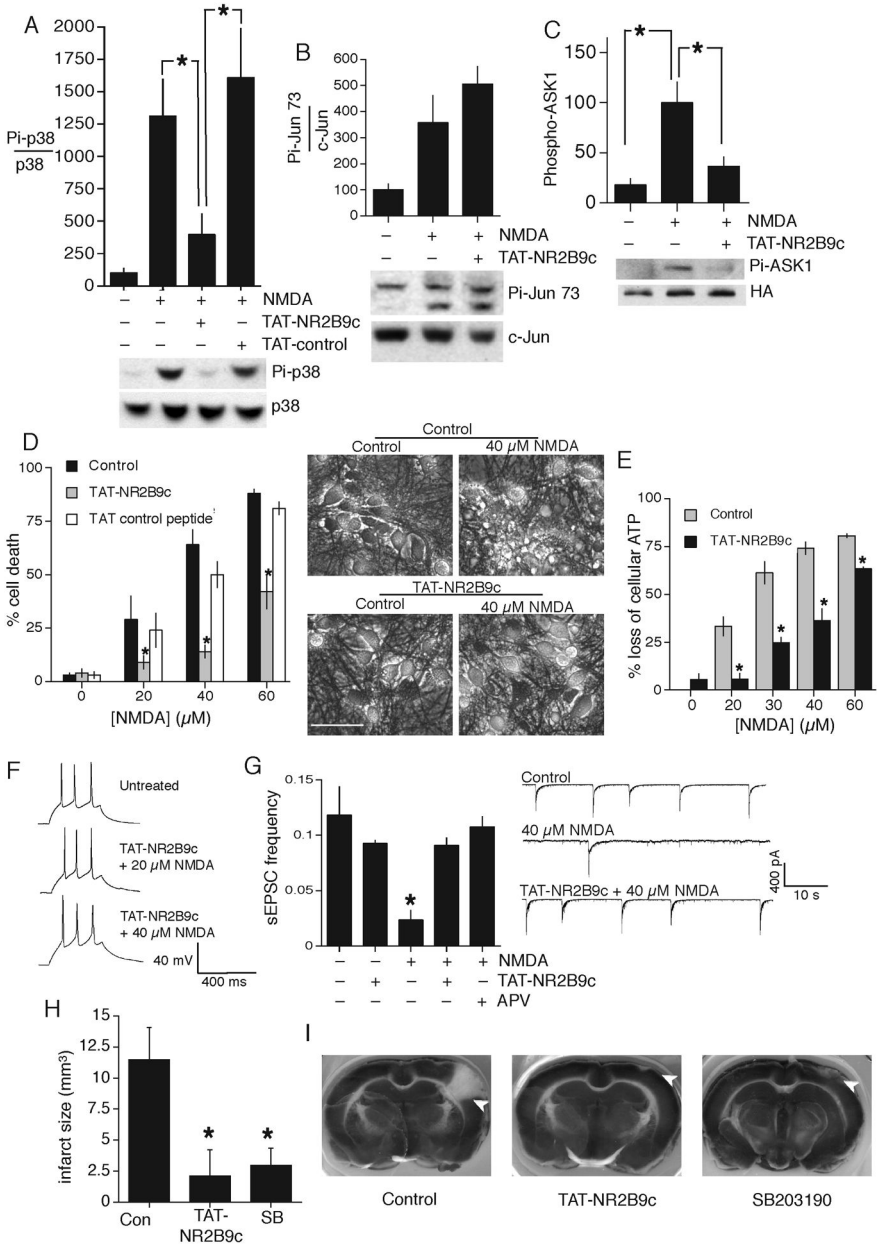

Fig. 4. NMDAR signaling to p38 MAPK in neurons is disrupted by a peptide mimetic of the NR2B PDZ ligand

A) TAT-NR2B9c uncouples the NMDAR from p38 activation. Western analysis of p38 activation in cortical neurons stimulated with NMDA (20 μM) for 5 min (*n* =6). All TAT-peptides were used in this study at 2 μM, cells pre-treated for 1 h. B) TAT-NR2B9c does not affect NMDAR-dependent JNK signaling. Western analysis of activation of JNK-dependent Jun phosphorylation in cortical neurons stimulated with NMDA (20 μM) for 30 min following and pre-treatment with TAT-NR2B9c (for 1 h) as indicated (*n* =3). C) TAT-NR2B9c uncouples the NMDAR from ASK1 activation. Neurons transfected with pHA-ASK1 and after 24 h stimulated with NMDA (20 μM) and pre-treated with vehicle or TAT-NR2B9c (*n* =3). HA-ASK1 was immunoprecipitated and subject to Western analysis of activation of ASK1, measured by analysing ASK1 (Thr-845) phosphorylation.D) TAT-NR2B9c protects neurons

against NMDAR-dependent excitotoxic cell death. Neurons treated with TAT-NR2B9c or control peptide for 1 h prior to excitotoxic insult (NMDA) for 1 h. (Left) Neuronal loss assessed after 24 h by DAPI staining and counting pyknotic nuclei (n =3). (Right) Phase-contrast pictures illustrating the protective effects of TAT-NR2B9c. Scale bar 50 μm. Note the phrase-bright cell debris from dead neurons in the control cultures treated with 40 μM NMDA (top-right). E) TAT-NR2B9c protects neurons against NMDAR-dependent excitotoxic cell death as assayed by loss of cellular ATP. Neurons treated as in (D) and after 24 h, cellular ATP levels measured by Cell-titer Glo assay (Promega, n=4). F) Neurons that are protected from NMDA toxicity by TAT-NR2B9c pre-treatment fire action potentials as normal. Neurons were treated as indicated using the same protocol as (D). 24 h after 40 μM NMDA exposure, surviving cells were patched under current clamp. Current was then injected (300 ms pulses at 1 Hz) until depolarized beyond −40 mV. Examples show the firing response that was triggered. G) Neurons that are protected from NMDA toxicity by TAT-NR2B9c pre-treatment experience normal levels of synaptic activity.Neurons treated as indicated using the same protocol as (D). 24 h after 40 μM NMDA (or vehicle) exposure, surviving cells were recorded under voltage-clamp. Spontaneous EPSC (sEPSC) frequency of the neurons was then measured over 3 min recording time (analysis shown on left, example traces on right).*p <0.05 compared to control neurons (n =7). H) TAT-NR2B9c and the p38 inhibitor SB202190 reduce infarct size in the 3 Pial Vessel Occlusion (3PVO) model of stroke. Adult rats treated with TAT-NR2B9c (7.5mg/kg) or the p38 inhibitor SB202190 (30 mg/kg) intravenously via a tail vein cannula 15 min prior to ischemia (3PVO-see methods). Animals were sacrificed 24 h post-ischemia and coronal brain slices taken for analysis of infarct size (n =8 for each group). I) Example brain slices (analysis in 4h) stained in 2% triphenyltetrazolium chloride and infarcts are highlighted with a white arrow.

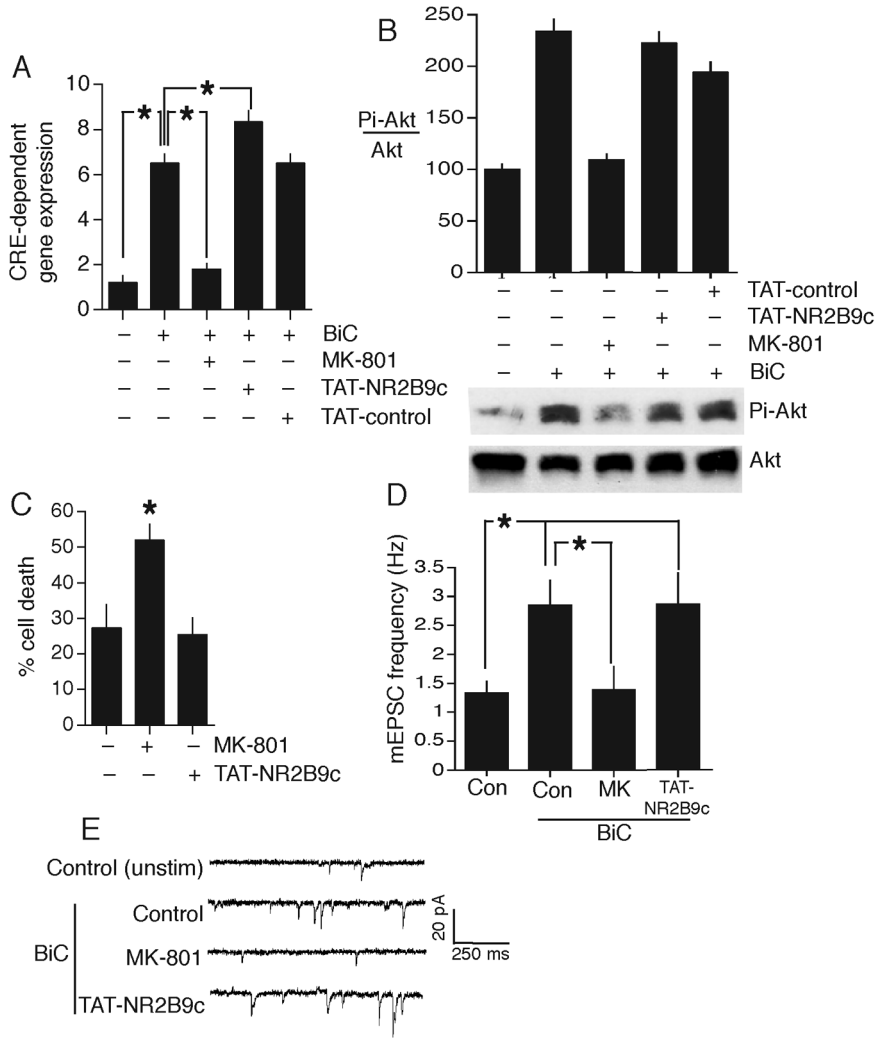

Fig. 5. TAT-NR2B9c does not block survival or plasticity signaling, unlike conventional NMDAR antagonists

A) TAT-NR2B9c does not impair synaptic NMDAR-dependent activation of a CRE reporter. Neurons were transfected with a CRE-Firefly luciferase vector plus pTK-renilla transfection control. 24 h post-transfection, neurons were pre-treated with the peptides (2 μM) or MK-801 (10 μM) for 1 h prior to bicuculline stimulation for 1h. After 1 h, synaptic activity was terminated by TTX (1 μM) and MK-801 (10 μM) and luciferase expression measured after a further 6-7 h. CRE-Firefly luciferase activity is normalized to Renilla control (*n* =3). B) TAT-NR2B9c does not impair synaptic NMDAR-dependent activation of Akt. Western analysis of Akt activation by bicuculline treatment, and the effect of the indicated peptides and drugs (*n* =3). C) TAT-NR2B9c does not promote neuronal apoptosis, unlike MK-801. Neurons were placed in trophically deprived medium and treated either with vehicle, MK-801 or TAT-NR2B9c for 72 h prior to fixation and DAPI staining. In the case of TAT-NR2B9c, fresh peptide was added every 24 h. The number of DAPI-stained apoptotic-like nuclei as a percentage of the total was calculated (*n* =4). D) TAT-NR2B9c does not block NMDAR-dependent synaptic plasticity. Hippocampal neurons were pre-treated for 1 h with peptide or MK-801 as indicated and in the presence of these compounds were treated with medium ± bicuculline for 15 min, then allowed to settle for 30 min. mEPSCs were then recorded for 5-10 min (minimum 300

events) and the frequency calculated (n =8-10 for each condition). E) Examples of traces used to generate the data shown in (D).

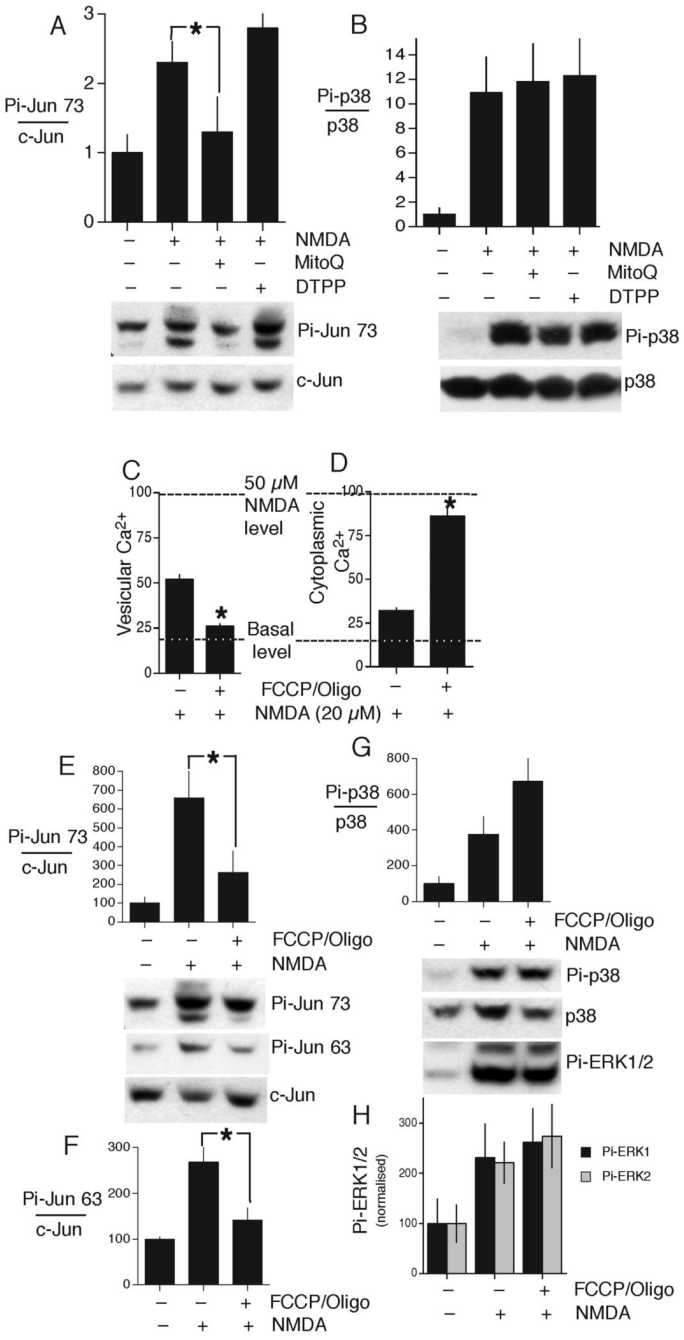

Fig. 6. JNK activation involves mitochondria

A,B) MitoQ blocks NMDAR-dependent JNK signaling, but not p38 activation. Western analysis of NMDAR-mediated JNK-dependent Jun phosphorylation (A) and p38 activation (B) in neurons pre-treated for 1 h with vehicle, MitoQ (5 μM) or DTPP control (5 μM) (n =4). C) Pre-depolarization of mitochondria blocks NMDA-induced vesicular Ca^{2+}uptake. Neurons were pre-treated (for 5 min) where indicated with FCCP+oligomycin (F/O) prior to stimulation and measurement of vesicular $^{45}Ca^{2+}$ uptake (n =3). D) Pre-depolarization of mitochondria causes an increase in NMDA-induced cytoplasmic Ca^{2+}load. Neurons were pre-treated where indicated with F/O prior to stimulation and measurement of cytoplasmic $^{45}Ca^{2+}$ uptake (n =3). For reference, level of cytoplasmic $^{45}Ca^{2+}$ uptake induced by 50 μM NMDA is also shown.

E-H) Pre-depolarization of mitochondria blocks JNK signaling but not p38 or ERK1/2. Assessment of the effect of F/O pretreatment on NMDA induction of c-Jun phosphorylation on Serine-73 (E, example blot below) c-Jun phosphorylation on Serine-63 (F, example blot above), both normalized to c-Jun levels (n =3), p38 activation (G, example blot below, n =3) and ERK1/2 phosphorylation (H, example blot above). Phosphorylation levels in (G) and (H) normalized to p38.

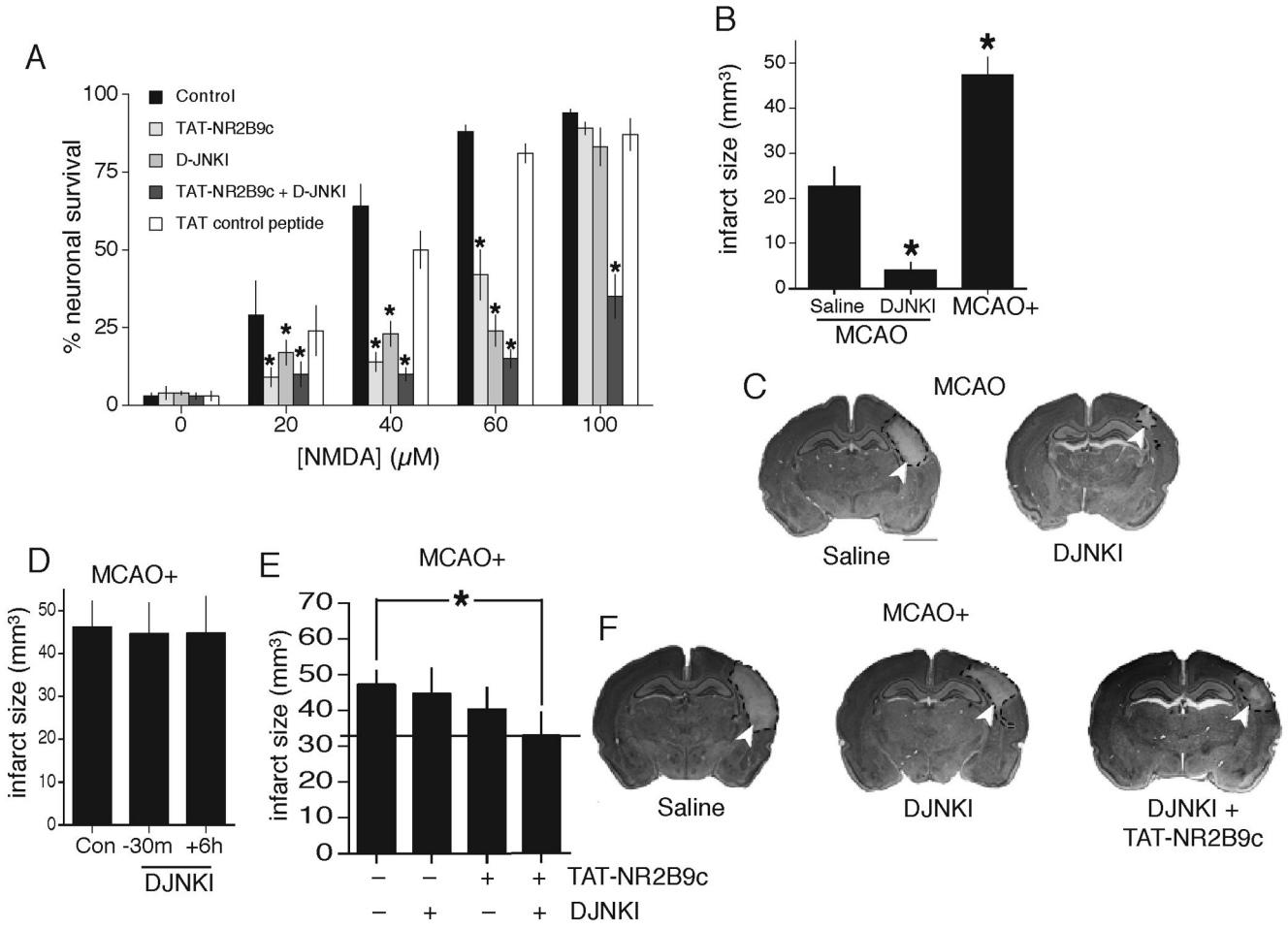

Fig. 7. Effective anti-excitotoxic therapy by combining TAT-NR2B9c with a TAT-fused JNK inhibitor *in vitro* and *in vivo*

A) TAT-NR2B9c and DJNKI1 are additively anti-excitotoxic in neurons *in vitro*. Cortical neurons pre-treated with the indicated peptides for 1 h prior to excitotoxic insult (NMDA) for 1 h. Neuronal loss assessed after 24 h (n=3). B) D-JNKI1 provides effective treatment of MCAO alone, and MCAO+ model results in large infarcts: Saline or D-JNKI1 (0.3mg/kg, i.p.) administered 6 h after simple MCAO (*, $p<0.001$, student t-test). For comparison, infarct size caused by severe (MCAO+, see methods) model of ischemia is shown. C) Examples of stained slices illustrating the protective effect of DJNKI1-see 7b. D) D-JNKI1 treatment of MCAO+ (MCAO + 90 min. carotid clamp). D-JNKI1 (0.3mg/kg, i.p. 6 h after MCAO or 30 min before it) does not significantly reduce the infarct volume. E) TAT-NR2B9c and DJNKI1 are additively protective in the severe MCAO+ stroke model. Combined peptide treatment of MCAO+. Neither D-JNKI1 (0.3mg/kg, i.p.) alone nor TAT-NR2B9c (7.5 mg/kg, i.p.) alone reduced the infarct volume significantly, but combined treatment with both peptides gave significant protection (**, $p<0.05$, Mann-Whitney test). For each treatment 7-20 animals were used. F) Examples of stained slices analyzed in 7e.